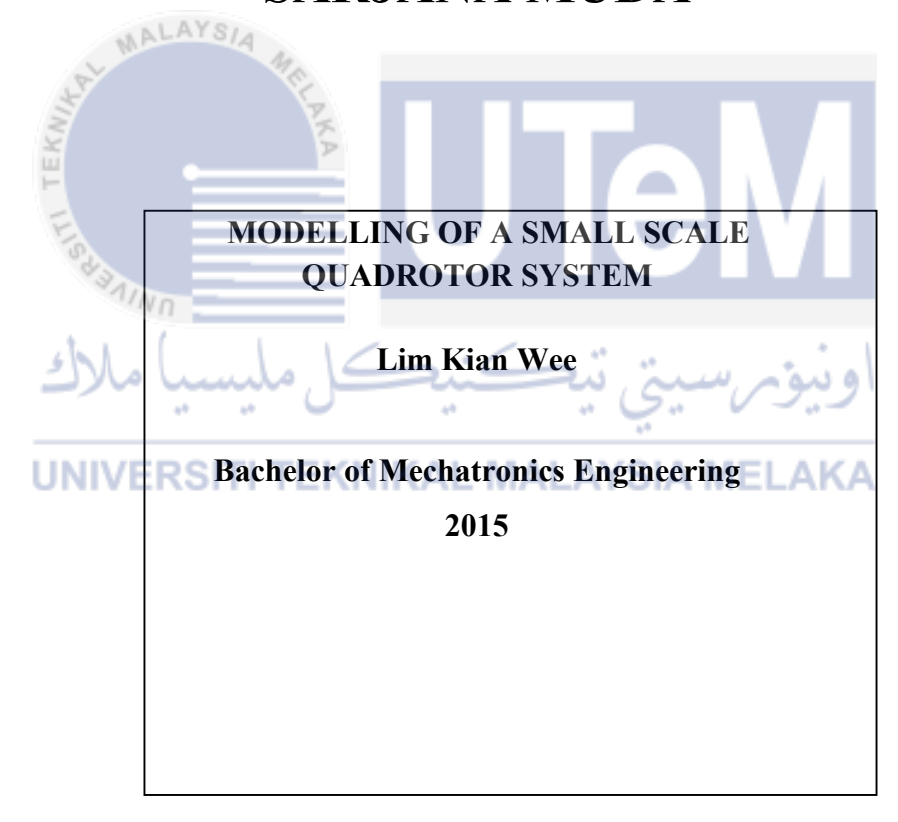


# FAKULTI KEJURUTERAAN ELEKTRIK UNIVERSITI TEKNIKAL MALAYSIA MELAKA

# LAPORAN PROJEK SARJANA MUDA



"I hereby declare that I have read through this report entitle "Modelling of	a Small So	cale
Quadrotor System" and found that it has comply the partial fulfillment for	awarding	the
degree of Bachelor of Mechatronics Engineering"		

EKNIK	PKA			
I ILIS	Signature			<u> </u>
BAINI	Supervisor's Nar	me :		
املاك	Date	ڪنيد	اسيتي تيه	اونيوم
UNIVE	RSITI TEKNI	KAL MAL	AYSIA MI	ELAKA

# MODELLING OF A SMALL SCALE QUADROTOR SYSTEM

# LIM KIAN WEE



A report submitted in partial fulfillment of the requirements for the degree of Mechatronics Engineering

Faculty of Electrical Engineering
UNIVERSITI TEKNIKAL MALAYSIA
MELAKA

I declare that this report entitle "Modelling of A Small Scale Quadrotor System" is the result of my own research except as cited in the references. The report has not been accepted for any degree and is not concurrently submitted in candidature of any other degree.

KNII	THE TOTAL PROPERTY OF THE PARTY
Signatu	re :
Name	
Date	اونيونرسيتي تيكنيكل مليس
UNIVER	SITI TEKNIKAL MALAYSIA MELAKA

# To my beloved mother and father



#### **ACKNOWLEDGEMENT**

Firstly, I am grateful that I have Madam Norafizah Binti Abas as my supervisor for my final year project who has been guiding me throughout the period of the final year project. I would like to thank her for her patience and motivation while guiding me to a better track of conducting this final year project. Her guidance on the report has helped a lot as she has the willingness to sacrifice her time on checking my report words by words. I would also very appreciate her as she always share her experience with us.

Secondly, I would like to thank Ms. Nur Maisarah Bt Mohd Sobran, who is my supervisor for my final year project. She had been guiding me a lot on the writing of the report. Furthermore, she has gave me encouragement and taught me the knowledge of writing the report of final year project.

Besides, I would like to thank my friends who are also the final year students that are under the supervision of Madam Norafizah Binti Abas. Throughout the period of this final year project, I am able to learn extra knowledge through other projects via discussion among each other. The discussion is very meaningful as the topic that is being discussed is quite challenging where every student able to exchange their opinion with each other. Thus, this has make the final year project more interesting.

Finally, I would like to thank my family who have been always giving support to me throughout the whole research of my final year project in University Teknikal Malaysia Melaka. Since the beginning of my studies here, they kept encourage me to do my best as this is the last project in my university life.

#### **ABSTRACT**

Surveillance is very important to ensure safety of a country. Lack of surveillance causes terrorist intrusion that happened in Lahad Datu, Sabah on 12 February 2013. Eastern Sabah Security Command (ESSCOM) was established by Department of Prime Minister for surveillance on the Eastern Sabah Security Zone (ESSZONE). The surveillance is done by the authorities of the ESSZONE which consist of ten districts. However, the limitation of the vision of a human and the large area for surveillance may decrease the efficiency of surveillance. Therefore, the Quadrotor is proposed for surveillance purpose due to it is a rotorcraft with four horizontal rotors which designed in square configuration. Despite of that, Quadrotor is a highly non-linear system and the difficulties on requiring the state space representation of the Quadrotor system. In order to overcome the problems faced, the objectives of this research are to perform computationally and physically modelling of the Quadrotor system and performing the analysis of the performance of the modelling of Quadrotor in terms of steady state error. The methodology is to compare both the model computationally and physically the Quadrotor system. The CAD drawing of the testbed is converted into SimMechanics Toolbox using SimMechanics Link add-on for the modelling computationally while modelling physically by conducting physical realization experiments. Total of three experiments such as the physical measurement, force-lift test and speed test, and bifilar pendulum experiment of Quadrotor are conducted to obtain related parameters for the Quadrotor system. The results of the experiments and the computed parameters form two state space representation. The analysis of each state space representation is done using MATLAB and tested as an open loop system. The physical modelling has a lower steady state error compared to computational modelling. These modelling are very important in order to produce an effective and accurate performance of the controller for Quadrotor system.

#### **ABSTRAK**

Kegiatan pengawasan adalah sangat penting untuk menjamin keselamatan negara. Kekurangan dari segi pengawasan akan menyebabkan pencerobohan pengganas yang telah berlaku di Lahad Datu, Sabah pada haribulan 12 Februari 2013. Eastern Sabah Security Command (ESSCOM) telah ditubuhkan oleh Jabatan Perdana Menteri untuk mengawasi Eastern Sabah Security Zone (ESSZONE). Pengawasan bagi sepuluh daerah ini dilakukan oleh pihak berkuasa. Walaubagaimanapun, keterbatasan manusia dari segi penglihatan dan kawasan di bawah pengawasan adalah sangat besar menyebabkan penurunan efisiensi dari segi kecekapan pengawasan. Oleh yang demikian, Quadrotor dicadangkan untuk menjalankan kegiatan pengawasan ini kerana ia adalah helikopter yang mempunyai empat pemutar yang mendatar dalam konfigurasi segi empat tepat persegi. Meskipun, *Quadrotor* merupakan sistem yang bukan linear dan mempunyai kesukaran untuk mencari sistem Quadrotor itu. Demi mengatasi masalah yang dihadapi, objektif kajian ini adalah untuk melakukan pemodelan secara komputasi and fizikal untuk sistem Quadrotor dan melakukan analisis prestasi pemodelan *Quadrotor* dari segi ralat keadaan mantap . Kaedah ini adalah untuk membandingkan kedua-dua model pengiraannya dan fizikal sistem Quadrotor. Lukisan CAD daripada Quadrotor itu ditukar kepada SimMechanics Toolbox menggunakan penambahan daripada SimMechanics Link untuk pemodelan pengiraannya manakala pemodelan fizikal dengan menjalankan eksperimen kesedaran fizikal. Sebanyak tiga eksperimen seperti pengukuran fizikal, ujian daya angkat dan ujian kelajuan, dan eksperimen bandul bifilar daripada Quadrotor dijalankan untuk mendapatkan parameter yang berkaitan untuk sistem Quadrotor itu. Keputusan eksperimen dan parameter digunakan untuk pengiraan dan membentuk dua perwakilan ruang keadaan. Analisis untuk setiap perwakilan ruang keadaan dilakukan dengan menggunakan MATLAB dan diuji sebagai sistem gelung terbuka. Pemodelan fizikal mempunyai ralat keadaan mantap yang lebih rendah berbanding dengan model pengkomputeran. Model ini adalah sangat penting untuk menghasilkan pengawal yang mempunyai prestasi yang berkesan dan tepat untuk sistem *Quadrotor*.

# **TABLE OF CONTENTS**

CHAPTER	TITLE	PAGE
	ACKNOWLEDGEMENT	ii
	ABSTRACT	iii
	TABLE OF CONTENTS	V
	LIST OF TABLES	viii
	LIST OF FIGURES	ix
	LIST OF APPENDICES	xi
1 . MA	INTRODUCTION	1
French	1.1 Research background	1
EK	1.2 Motivation and significant of research	3
	1.3 Problem statement	4
(SP)	1.4 Objective	5
- 10	1.5 Scope	5
ملاك	1.6 Report outline	6
UNIVE	LITERATURE REVIEW	8
	2.1 Theories and basic principles	8
	2.1.1 Newton-Euler formulation method	8
	2.1.2 SimMechanics Toolbox	9
	2.1.3 SimMechanics Link	10
	2.2 Review of Previous Related Works	11
	2.2.1 Method of Modelling	11
	2.2.2 Overall System	12
	2.2.3 Experiments Conducted	17
	2.3 Summary and Discussion of the Review	19

3	METHODOLOGY	23
	3.1 Project Overview	23
	3.2 Testbed's Components	25
	3.2.1 Motor	25
	3.2.2 Propeller	25
	3.2.3 Framework	26
	3.2.4 Platform	26
	3.2.5 IMU	27
	3.3 Derivation of Mathematical Modelling	27
	3.3.1 Dynamic Modelling of Quadrotor	27
	3.3.2 State Variables of Quadrotor	28
	3.3.3 Kinematics of Quadrotor	29
	3.3.4 Dynamics of Rigid Body	30
AL MAL	3.3.5 Moment of Inertia of Quadrotor	31
AN A	3.3.6 Force and Moments	33
TEX	3.4 Computational Modelling	36
E	3.4.1 Solidworks	38
NIVER	3.4.2 SimMechanics Link	38
ch 1	3.4.3 SimMechanics Toolbox	39
ا مالاك	3.5 Experiments Conducted	41
LINUVEE	3.5.1 Physical Measurements	41
UNIVER	3.5.2 Force-life and Rotor's Speed Test	42
	3.5.3 Bifilar Pendulum Experiment	43
	3.6 Analysis of Modelling	45
4	RESULT AND DISCUSSION	46
	4.1 Introduction	46
	4.2 Results of Computational Modelling	46
	4.2.1 Assembly of Testbed	46
	4.2.2 The Block Diagram	48
	4.2.3 Analysis of the Testbed	49
	4.2.4 Mathematical Model of Quadrotor	52
	4.3 Results of Physical Realisation Experiments	54

4.3.1 Physical Measurement Results	54
4.3.2 Results of Force-lift and Rotor's Speed	55
Test	59
4.3.2.1 Motor 1	56
4.3.2.2 Motor 2	58
4.3.2.3 Motor 3	60
4.3.2.4 Motor 4	62
4.3.3 Results of Bifilar Pendulum Experiment	65
4.3.4 Mathematical Model of Quadrotor	68
4.4 Analysis for Mathematical Model of	69
Quadrotor	
4.4.1 Computationally Method of	69
Mathematical Modelling	
4.4,2 Physically Method of Mathematical	72
Modelling	
4.4.3 Comparison for the Outputs	75
5 CONCLUSION	77
5.1 Conclusion	77
5.2 Suggestion for Future Work	78
REFERENCES REFERENCES	79
APPENDICES	82

# LIST OF TABLES

<b>TABLE</b>	TITLE	PAGE
2.1	The summary of each journal	19
2.2	The methods and the hardware configuration for this project	21
4.1	List of components used in Testbed	47
4.2	Force generated with given angular velocity	51
4.3	Results of the simulation on testing the thrust force and drag force	52
4.4	The physical measurement of the respective components based on	54
	description	
4.5	The results of force-lift test for motor 1	56
4.6	Results of the simulation on testing the thrust force for Motor 1	57
4.7	The results of the force-lift test for motor 2	58
4.8	Results of the simulation on testing the thrust force for Motor 2	59
4.9	The results of the force-lift test for motor 3	60
4.10	Results of the simulation on testing the thrust force for Motor 3	61
4.11	The results of the force-lift test for motor 4	62
4.12	Results of the simulation on testing the thrust force for Motor 4	63
4.13	Result of the Force-Lift Test	64
4.14	Result of the Bifilar Pendulum Experiment	65
4.15	The moment of Inertia through calculation and theoretically	67

# LIST OF FIGURES

<b>FIGURE</b>	TITLE	PAGE
1.1	Convertawings Model A. First Quadrotor that able to fly	2
1.2	Percentage of images incorrectly identified for four stimulus	3
	conditions with standard error bars.	
2.1	Coordinate System of Quadrotor	12
2.2	The X-shaped Unmanned Aerial Vehicle, Quadrotor	13
2.3	The top view of a + shaped Quadrotor	14
2.4	The movements of the Quadrotor	14
2.5	The dynamics of Quadrotor	15
3.1	Overall project flowchart	24
3.2	Definition of Axes	28
3.3	An assumption of a Quadrotor shape for derivation of inertia	31
3.4	The definition of forces and torques acting on the motors of the	33
-	Quadrotor Level Quadrotor	
3.5	The process for Computational Modelling	37
3.6	The flowchart of the process in SimMechanics Toolbox	40
4.1	The assembly of the Quadrotor	47
4.2	The block diagram after the conversion from Solidwork	48
4.3	The mass properties of the testbed Quadrotor	49
4.4	Result for one of the flow simulation test	50
4.5	The graph of Force against Duty Cycle Computationally	51
4.6	The graph of Force against Duty Cycle for Motor 1	57
4.7	The graph of angular velocity against the duty cycle of motor 1	57
4.8	The graph of force against the duty cycle of motor 2	59
4.9	The graph of angular velocity against the duty cycle for motor	59
	2	
4.10	The graph of force against the duty cycle of motor 3	61

4.11	The graph of angular velocity against the duty cycle for motor	61
	3	
4.12	The graph of force against the duty cycle for motor 4	63
4.13	The graph of the angular velocity against the duty cycle of	63
	motor 4	
4.14	The graph of yaw of the Quadrotor system	65
4.15	The graph of output and input in pitch movement for	70
	computational modelling	
4.16	The graph of output and input in yaw movement for	70
	computational modelling	
4.17	The graph of output and input in roll movement for	70
	computational modelling	
4.18	The graph of output and input in z direction for computational	71
	modelling	
4.19	The graph of output and input in y direction for computational	71
	modelling	
4.20	The graph of output and input in x direction for computational	71
	modelling	
4.21	The graph of output and input in pitch movement for physical	73
	modelling	
4.22	The graph of output and input in yaw movement for physical	73
	modelling	
4.23	The graph of output and input in roll movement for physical	73
	modelling	
4.24	The graph of output and input in z direction for physical	74
	modelling	
4.25	The graph of output and input in y direction for physical	74
	modelling	
4.26	The graph of output and input in x direction for physical	74
	modelling	

# LIST OF APPENDICES

APPENDIX	TITLE	PAGE
A	Gantt Chart of the Research	82
В	The sketch of the testbench used in Bifilar	83
	Pendulum Experiment with the dimensions.	
C	The components of the Quadrotor with	84
	dimensions.	
D	Coding in MATLAB for modelling	86
	computationally	
E	Block diagram of the open loop system of	87
N. C.	modelling computationally	
FΞ	Coding in MATLAB for modelling physically	88
G	Block diagram of the open loop system of	89
SHIN	modelling physically	
للاك	ونيوسيتي تيكنيكل مليسياً ه	\
UNIV	ERSITI TEKNIKAL MALAYSIA MELAKA	Į.

#### **CHAPTER 1**

#### INTRODUCTION

# 1.1 Research Background

In this modern era of globalisation, there are many kinds of technologies have been invented to ease the daily routine of humans. There are technologies which are able to fly by its own using four rotors. These type of vehicle is called as Quadrotor. Quadrotor are known as Quadcopter which is a helicopter that consists of multi-rotor. Typically, it is lifted and propelled by four rotors. There are many functions of this Quadrotor that are used by a lot of people such as the army, the police and other related person. This vehicle can be used for surveillance, search and rescue operation and many more. This is due to the size of the Quadrotor is small and easily controlled. It is normally has a camera fixed on it so that the person in charge able to see the surroundings of the Quadrotor. As in general, autopilot for Quadrotor is optimal. This vehicle is able to be used as load transportation from one place to another by just setting the location of destination. Developing a Quadrotor is not an easy task like creating a normal robot. Many things are taken into account such as the physical mathematical modelling of the Quadrotor, the parameter of the variables of the Quadrotor and even the configuration of the Quadrotor. The modelling of the Quadrotor is very important as the performance of the developed controller is depending on how well is the modelling [1].

In the early days of the history of flight, the configurations of a Quadrotor are seen as the solution to fix the persistent problems with vertical flight which means that the control of torque that being induced are being ignored by the counter-rotation and the comparatively short blades which could be constructed easily. The first Quadrotor has been invented on the year 1922 that is called as Oemichen No. 2 and follow by the De Bothezat Quadrotor which is built in 21<sup>st</sup> February 1923. Unfortunately, the first two Quadrotor are unable to lift off

due to its physical configuration. The first Quadrotor that manage to lift off and fly is the Convertawings Model A, built on 1955/1956. The first flight is on the March 1956.



Figure 1.1: Convertawings Model A. First Quadrotor that able to fly [2]

This Quadrotor is among the most successful Vertical Take Off and Landing (VTOL) vehicles. At first, like any other prototype, it had a poor performance and also requires more pilot work load. This has led to poor stability augmentation and also imperfect control authority. In comparison with other prototypes of these vehicles, this kind of Quadrotor has quite a huge weight difference which is including the weight of the pilot. The material used to build this prototype should be light in order to decrease the overall weight of the prototype so that the vehicle can easily lifted off vertically and also decreasing the stress on the rotor.

Quadrotor lies under the group of Unmanned Aerial Vehicle (UAV). This vehicle is an aircraft without a human pilot on-board and is usually controlled either autonomously by on-board computers or by a remote control of a pilot on somewhere else. Nowadays, there is a UAV that is quite popular and on demand which is the Quadrotor. It can be controlled either using an electronic control system or electronic sensor to stabilize the prototype from being crashed onto any obstacles which enables the Quadrotor to fly in indoor or outdoor places.

# 1.2 Motivation and Significance of Research

The terrorist intrusion in Lahad Datu, Sabah which is happened on 12 February 2013 has caused a big worrisome of Malaysian on their safety. The solution for this case is that the Eastern Sabah Security Command (ESSCOM) was established by the Department of Prime Minister. This department is a security enforcement agency whereby the Eastern Sabah Security Zone (ESSZONE) kept under surveillance of them in order to strengthen the protection and security in the east cost of the state. This ESSZONE covers 10 districts with a distance of 1733.7 km of the east coast of Sabah namely, Tawau, Semporna, Kunak, Lahad Datu, Kinabatangan, Sandakan, Pitas, BCS, Kota Marudu and Kudat.

Although the Police Headquarters has given order to strengthen their surveillance on the respective areas, they cannot be as efficient as expected due to human behaviours such as limited eyesight vision for the surveillance job. This is the limitation in surveillance techniques as it should cover wide area of east coast of Sabah [3].

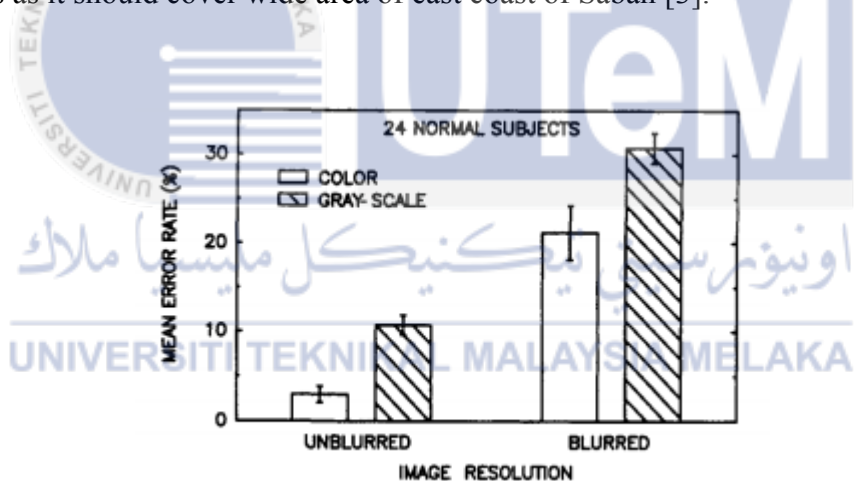


Figure 1.2: Percentage of images incorrectly identified for four stimulus conditions with standard error bars [3].

The Figure 1.2 shows the limitation of the vision of humans for four stimulus conditions that able to be relate to the surveillance on the east coast of Sabah. Since there is limitation of the vision of humans, this indicates the weakness of the current surveillance techniques.

### 1.3 Problem Statement

Based on the motivation, flying vehicle is proposed in order to overcome the limitation faced. Normally, flying vehicle used is the helicopter but there are limitations of the usage of the helicopter. The helicopter requires mechanical linkages to differ the rotor blade pitch angle as they rotates. The propeller of the helicopter is large in diameter which increases the work load for each rotor and experiences more stress. Due to the limitations of the helicopter, Quadrotor is proposed to overcome the limitations faced by the helicopter and the limitation in surveillance technique. The Quadrotor is a highly nonlinear system where the system does not produce an output that is not directly proportional to the given input. In other words, it contains a system that requires a crucial modelling so that it can controlled robustly. The problem faced when developing a plant which is finding a suitable state space representation that suits the system of the Quadrotor. Many variables of the Quadrotor such as the configuration of the Quadrotor should be taken into account on developing the mathematical modelling. For example, the configuration of the Quadrotor is the configuration of the body frame, the desired movement of the Quadrotor, the size of every each rotor, the overall weight of the Quadrotor and other variables. Besides, there some of the variables that are unable to be calculated easily. In fact, developing a mathematical modelling is important as the performance of the controller to be developed depends on how well is the mathematical model being developed. Furthermore, there are problems with the IMU such as the accelerometers and the gyroscopes. The accelerometer measures all forces that are working on the object. It also measures a lot more than just measuring the gravity vector. Any small vibration acting on the object will disturb the measurement completely. On the other hand, the gyroscopes has the measurement that has high tendency to drift which does not return to zero when the system is back to its original position. Thus, the more variables of the Quadrotor are taken into account, it is expected to produce a better and efficient transfer function that represents the modelling of the prototype [1].

# 1.4 Objective

This objectives of this research are:-

- 1.4.1 To computationally model the Quadrotor system using SimMechanics Toolbox and Solidworks.
- 1.4.2 To physically model the Quadrotor system using physical realisation experiments.
- 1.4.3 To analyse the performance of modelling of Quadrotor in terms of steady state error.

## 1.5 Scope

The scopes of this research are:-

- The testbed of this Quadrotor is developed by previous student, Ahmad Mahadi bin Razali.
- Newton-Euler formulation is used to derive the mathematical modelling of the Quadrotor system.
- The MATLAB Simulink environment is used to develop the modelling using functional blocks and it is developed using SimMechanics and Simulink functional blocks only but not using blocks from other toolboxes.
- The development of the modelling of the Quadrotor will be assumed to be at closed and indoor area which is in the laboratory whereby the weather of the surrounding will be ignored.
- The physical realisation experiments conducted consist of four experiments only which are the physical measurement, force-lift and speed test, and bifilar pendulum experiment.
- The analysis of performance of modelling of Quadrotor system is tested for the steady state error only. The transient response is not tested in this research.

# 1.6 Report Outline

This project report consists of five main chapters excluding the references part. It begins with introduction, followed by literature review, then research methodology, and preliminary result and lastly the conclusion for the overall project.

In Chapter 1, the introduction starts with the research background which includes the motivation and the significance of the project, the problem statement to be solved during this project, the objectives of doing this project and the expected project outcome. The first part is the explanation of what is the title of the project and the understanding of the hardware. This part is need to blend in together with the motivation and the significance of the research. For the next part, the problem statement is the part where problems occurred will be stated out and some expected methodology to solve the problem which also includes some of the expected result. The objectives is to state out what should be done throughout the whole project. Finally is the expected project outcome which is also known as the expected result for this project.

In chapter 2, the literature review is divided into three parts which is the theory and basic principles, the review of the previous related works and ended up with the summary and discussion of the whole review. The first part is the understanding and the explanation of the used theories and basic principles throughout the project. It is followed by the review of the previous related works whereby this part is to review back some journals which is related to the project title and give some summary on the journals. Lastly, the summary part is to conclude and compare all the reviewed journals and come out with a final conclusion.

In Chapter 3, the research methodology consists of four parts which is the principles of the methods or the techniques used in the previous work, some detailed discussion on the selected techniques and approach used such as the analytical or modelling and simulation, description of the work to be simulated. The first part is for discussion and analysing the principles of the techniques or methods used in the previous related works such as journals. Then, it is followed by some detailed discussion on the chosen techniques by using either analytical which is the statistics or by using modelling and simulation. Next, some of the set-

up of the experiment and data collection will be determined. Finally, project Gantt chart and key milestones are developed for making sure the path of this final year project is correct.

In Chapter 4, the preliminary results has two equally important subtopics which is the project achievement and the future work planning for the upcoming Final Year Project 2 (PSM2). This chapter started with the explanation on the achievement of the project itself by highlighting the initial results which have been achieved this far either can be the data collection, simulations of modelling and some simple analytical analysis on the performance.

Lastly, the last main chapter which is the overall conclusion for this final year project. This part is to conclude every each chapter previously on what has been done. Besides that, this chapter should also include some of every subtopics that have been discussed in details and clear.



#### **CHAPTER 2**

#### LITERATURE REVIEW

This part discusses the published information regarding the Quadrotor within a certain time period. It is just a simple summary of the sources related to the title. This part of report covers the explanations about the theories and the basic principles. Besides, this part also includes the review of previous related works which give a new ideas that is taken from a few different journals. This part is concluded up with the summary of the overall literature review and also the discussion of the review and the choice of the subsections to be used throughout this final year project.

# 2.1 Theories and Basic Principles

In this part of the theory and basic principles, the theory of Newton-Euler formulation is being discussed in details together with an example for a better understanding. Besides, the principle of the SimMechanics is briefly highlighting its usage and functions of every each functional block which is available in MATLAB Simulink environment.

#### 2.1.1 Newton-Euler formulation method

This Newton-Euler formulation method is used to obtain a linear, angular accelerations and velocities for each link, free-body diagrams and Euler equations and Newton's Law. The motion of a rigid body can be disintegrated into translational motion with relative to an arbitrary point which is fixed to the respective rigid body and the same goes to the rotational motion is relative about that point.

According to Mark D. Ardema [5], the dynamic equation is represented with two equations where one describes the translational motion of the centroid, which can be said as the centre of mass, and the other one describes the rotational motion about the centroid. The author added that Newton-Euler method uses the propagation formulas for position or orientation of links and it consists outward iterations for velocities and accelerations.

Newton-Euler algorithm has computational complexity which means there are no any iteration or loops, the computation of the sets of equations are performed only once and the number of additions and multiplications is proportional to the number of links. It can be adapted for any serial manipulators with prismatic (P), rotary (R), or any other joints such as spherical and gimbal joints. Used for symbolic computation of equations of motion of a hardware. Typically, this method is used in development of robotics.

Based on Jerry Ginsberg [6], Newton-Euler method is the balance of forces or torques where its equations are written separately for each body. It represents the inverse dynamics in the real time where it is the best for synthesising of a model-based control schemes while the equations are assessed in recursive and numeric way. The closed-form dynamic equations which is identical to the Euler-Lagrange method can be done by eliminating the reaction force and the back-substitution of expressions.

# 2.1.2 SimMechanics

SimMechanics is a toolbox of Simulink environment which is used to model and simulate multi-body mechanical systems especially for 3D mechanical systems such as unmanned aerial vehicle, robots and many more. In this toolbox, model of the multi-body system can be developed easily using blocks to represents the bodies, joints, constraints and force elements. This toolbox will then formulates and solves the equation of motion for the developed mechanical model. Models from the CAD systems can be imported into SimMechanics including the mass, inertia, joint, constraint and 3D geometry of the models of CAD systems. The previous step can be done by using the add-on by using SimMechanics Link on the Solidwork software. 3D animation of the system dynamics will be automatically generated. The models can be parameterized using MATLAB variables and expressions. The

models also can be used to design the control systems or the multi-body system in Simulink. Furthermore, other toolbox which is included in Simscape toolbox such as electrical, pneumatic, hydraulic and other components into the mechanical model and able to test them in a single simulation environment. The developed model can also deployed to other simulation environments including SimMechanics support C-code generation using Simulink Coder and handware-in-loop (HIL) systems. There is a block library for this SimMechanics. It provides blocks such as body elements, joints, utilities and others. Body elements is representing the solid properties of a rigid body which able to initialise its moment of inertia and mass. The constraints block is used to constrain the relative motion between two rigid body elements. This is the same as the joints where it represents the mechanical degree of freedom between two rigid body frames. The forces and torques blocks is used to apply any internal or external forces and torques between two rigid body. Lastly, the gears and couplings blocks is to couple the motion of two rigid body [7].

# 2.1.3 SimMechanics Link



SimMechanics Link is an utility that bridges the gap between geometric modelling and block diagram modelling and simulation, with the combination of Simulink and SimMechanics software with CAD. With this utility, the SimMechanics model can be created from a CAD assembly by exporting CAD assemblies into physical modelling XML file. This file can be imported to generate a SimMechanics model automatically. Besides, the translation of CAD translation assemblies into dynamic block diagram models. The things that is being export is the CAD assemblies into physical modelling XML format which captures the mass and moment of inertia for every part in the assembly and the constrains definitions between parts. In addition, the graphic files that defines the body geometries of the assembly part is also being exported. Next step is by importing the physical modelling XML for the generation of SimMechanics models. The XML representations of parts and constrains is converted onto bodies and joints in SimMechanics model where the generated model uses the exported body geometry graphics to visualize the bodies [8].

#### 2.2 Review of Previous Related Works

This part discussed the previous related work to this final year project. All the related journals are being reviewed and being synthesize and summarize in terms of their configuration and characteristics of the related works.

## 2.2.1 Method of modelling

There are many types of method of modelling are being used to represents the plants of a system. Typically, the method such as Newton-Euler equations and Euler-Lagrange equations are normally being used to model the mathematical equation of the hardware. The usage of the Newton-Euler formulation equations is increasingly used due to its function on evaluating and developing the equations on the modelling of a hardware. The followings are all reviews and the steps on applying the equations in their research. According to Jiang J., et. al. [9], they uses the Newton-Euler equation as the choice of method of modelling the hardware rather than Lagrangian method. This is due to that the equation which represents the translation movement is neglected and the equations developed using Newton-Euler equation can be used easier compared to other methods for the model movement such as roll, pitch and yaw movements. Most important of all is that modelling of a model is very important before developing any control. In fact, the better the hardware is being modelled, the better condition of the control is being developed. Besides, Aleksandar R. et. al. [10] and Fernando, H.C.T.E. et. al. [11] used Newton-Euler method describe the motion of a six degree-of-freedom rigid body and it is defined with two reference frames which is the earth inertial frame and the body fixed frame for controlling the movement of the model and to model the Quadrotor dynamics whereby it predicts the effects of the forces and torques generated by the four propellers on the Quadrotor motion respectively. Besides, Deepak G. et. al. [12] used the same method for derivation of mathematical model before producing PID using self-tuning fuzzy algorithm. The Figure 2.1 is the proposed coordinate system.

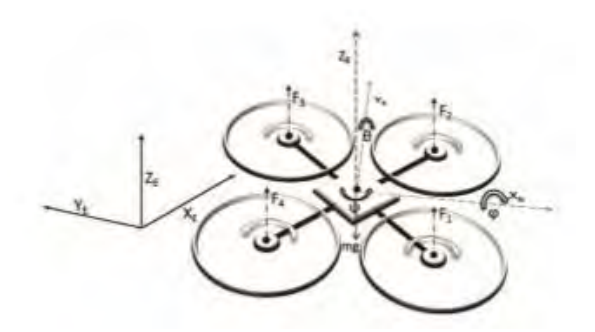


Figure 2.1: Coordinate System of Quadrotor [12]

The body frame is based on the inertial frame by a position vector (x,y,z) and three Euler angles  $(\phi,\theta,\psi)$  which represents the roll, pitch and yaw angle respectively.

On the other hand, Euler-Lagrange method is used by Yogianandh N.et. al. [13] and Mostafa M. et. al. [14] to define equations of motion for six degree-of-freedom system and to develop the mathematical dynamic model of the vehicle and they insisted that the modelling is essential for designing a good controller respectively. The author Yogianandh N.et. al. is then The developed modelling is then drawn using MATLAB Simulink. The derived model is simulated to determine the behaviour of the Quadrotor. From the developed model, they developed a control strategy using linear PD controllers while the other author is then determine the dynamic equation of the body and specify the structure of uncertain dynamics. The relationship between the inputs and outputs of the control should be determined and also defining the dynamic of the actuators.

### 2.2.2 Overall System

Nowadays, there are many kinds of Unmanned Aerial Vehicle are being constructed in many different configuration. The configuration of the body of the hardware and the movement of the Quadrotor is being discussed in details together with the review of previous related work.

There are two types of configuration of the body frame of the Quadrotor is developed nowadays, which is the X-shaped body frame configuration and the + shaped body frame

configuration. This configuration may affect the development of the equation of the mathematical modelling of the Quadrotor by giving different amount of length and the mass which is used in derivation of input equation. According to Yang J. P. et. al. [15], the Quadrotor of them consists of four fixed pitch angle rotors which is powered by four electronic motors which are mounted at the end of an X-shaped frame. The Quadrotor consist of four subsystems, airframe, flight control system and power system. Figure 2.2 is the Quadrotor they have developed. The main model parameters are identified through CFD while the rolling and pitching moments of inertia are measured accordingly.



Figure 2.2: The X-shaped Unmanned Aerial Vehicle, Quadrotor [15]

On the other hand, based on Yasir A. et. al. [16], the Quadrotor used by them is also consists of four dc motors on which the propellers are mounted but it is arrange at the corners of a + shaped frame, where all the arms make an angle of 90 degrees with one another. The Figure 2.3 is the Quadrotor they have developed. During development of the model, there are certainly some assumptions to be made such as the propellers and the Quadrotor body is rigid, the design of the frame is symmetrical, no air friction on the body frame and zero free stream air velocity.

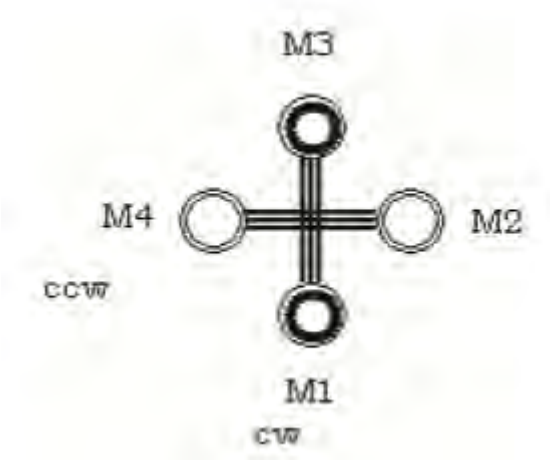


Figure 2.3: The top view of a + shaped Quadrotor [16]

The movement of the Quadrotor is being discussed with the previous related journal such that there are many types of movement of the Quadrotor such as yaw, pitch, vertical, roll and throttle. These characteristics also depending on the body frame configuration. The mathematical modelling development will affect the movement of the Quadrotor.

Furthermore, based on Deepak G. et. al. [12], they use a cross-shaped aerial vehicle which is the Quadrotor and it's capable on taking off vertically and landing. It consist of four motors where each is mounted per corner equidistant from the centre. Most importantly is that they insisted on the synchronized rotational speed of all the motors to control the movement of the Quadrotor such as the yaw, pitch and direction of the Quadrotor. Figure 2.4 shows the abilities of the movement of the Quadrotor.

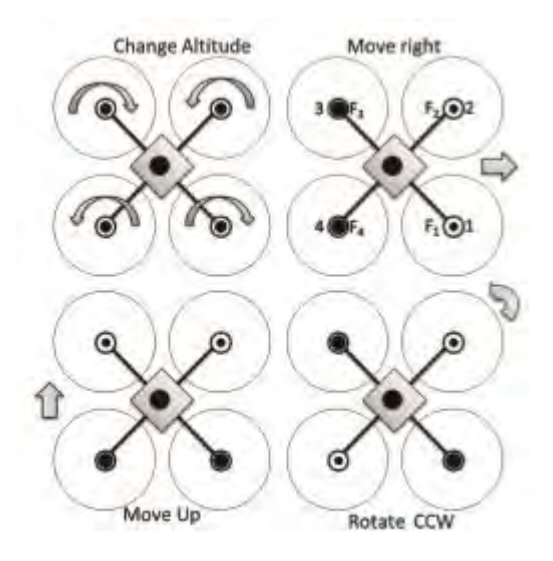
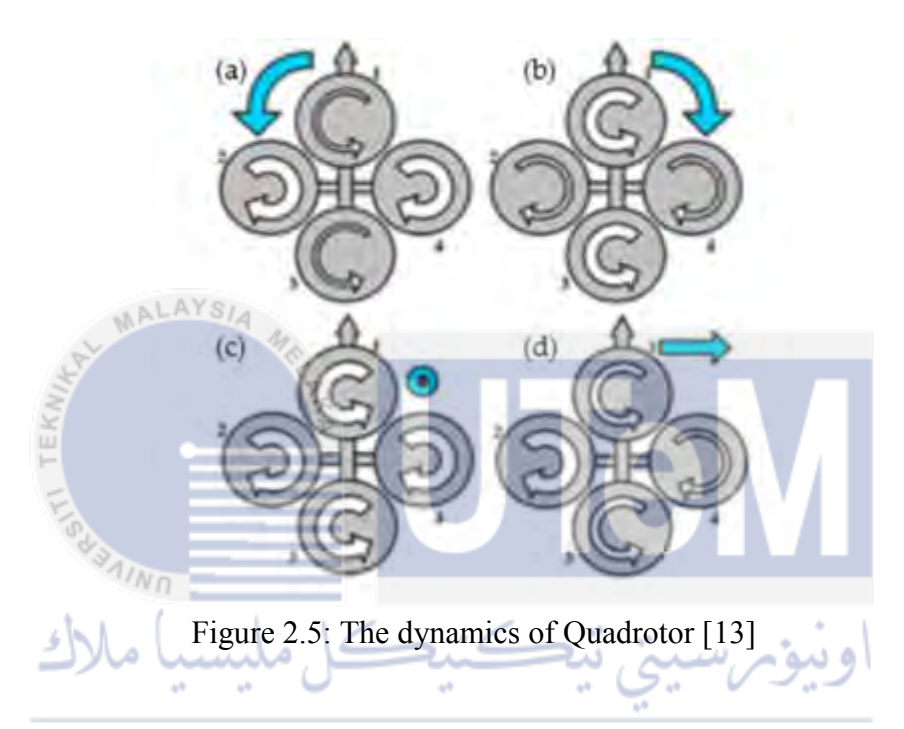


Figure 2.4: The movements of the Quadrotor [5]

Based on Yogianandh N. et. al. [13], a Quadrotor lies within their rotors. The payload and the flight time performance of the aircraft are all depend on the specifications of the batteries, motors and the propellers. In fact, the most influential components of the Quadrotor which affect the most is the rotors that is able to influence the natural dynamics and power efficiency of the vehicle. There are some assumptions made during the modelling which is that the motor dynamics are too fast and therefore neglected and the rotor blades are assumed perfectly rigid so there will no blade flapping occurs.



The figure (a) and (b) in Figure 2.5 shows the difference in the torque of each propeller to manipulate the yaw angle while figure (c) is the hovering motion and vertical propulsion due to balanced torque of each propeller. Meanwhile, figure (d) shows the difference in thrust to manipulate the pitch angle and the roll angle.

On the other hand, the propeller is also an important component in the Quadrotor. Ameho, Y et. al. [17] stated that the important phenomenon to the blade flapping dynamics and rotor drag. They considered using two-blade propeller in forward flight, the blade advancing in the same direction as the vehicle has a greater aerodynamic speed than the opposite blade. The lift created by a profile is proportional to the square of the aerodynamic speed for both blades which are not subjected to the same efforts. The blades will bend asymmetrically along a rotation lead to inducing the blade flapping dynamics.

Besides, Shah, K et. al. [18] stated that the usage of the propellers is to generate aerodynamic lift force. They used two pairs of propellers where a pair of it rotates clockwise and the other pair rotates anti-clockwise to nullify the gyroscopic effect of each individual motor. They used the propellers with a diameter of 11 inches and pitch of 4.7 inches/revolution.

According to Orsag, M. et. al. [19], they state that most of the research use DC motors as the driver of the rotors. Although new designs often use brushless DC motors, brushed motors are still used due to it's lower cost compared to others. Though, brushless DC motors have advantages compared to brushed DC motors where is produce more torque per weight, more torque per watt to increase its efficiency and increased reliability. Thus, they ended up using standard brushed DC motor due to its advantages above. From the motor, they came out the result of its rotation speed, induced speed and thrust of the motor with a given range of voltages.

In addition, Edward, P. et. al. [20] uses JETI Phasor 30/3 hobby aircraft brushless motors to drive the rotors which consists of six-pole, 18-stator-coil and is designed for direct propeller drive without the need of a gearbox. This type of motor is chosen due to its maximum power rating of 350W, high-torque performance, low speed and availability during that time. The motors are sensorless and it must be electronically commutated via back-EMF or with external sensors. The motors are mounted on pods that screw onto the carbon-fibre arms and can be shimmed for the motor axis to be tilted side to side. Each motor weighs 290g and size of 35x55 mm.

The motor driver normally used is the Electronic Speed Control (ESC). Based on Tefay, B. et. al.[21], they used FPGA-based electronic speed control (ESC) for driving brushless DC electronic motors terminal voltages as it allows for sensing, computation and consist a higher control bandwidth. It contains three MOSFET half-bridges. Pulse Width Modulation (PWM) is only applied onto the low side MOSFETs. The position sensing algorithm of the rotor is not affected by the given PWM pattern where the pattern was to reduce switching losses and match the commercial ESCs for comparison. For open loop ramping, the ESC operates the motor using open loop control to accelerate the rotor with a sufficient speed to sense the position of rotor. Basically, 16% duty cycle are able to generate enough torque to drive almost all DC motors.

## 2.2.3 Experiments Conducted

For physical realisation experiments, Güçlü, A. [22] carries out three experiments which are the physical measurement, speed test and the bifilar pendulum experiment respectively. These experiments are conducted to determine the speed of the motor, propeller as well as the moment of inertia of the Quadrotor.

The experiment of measuring the propeller angular velocities are being carried out first then following by the mathematical calculation for obtaining the thrust force. After this, another calculation is carried out to obtain the motor thrust force by using a weighing device directly. A hand type of tachometer is used to measure the angular velocity of the propellers. This device is to display the angular velocity of the propeller. The angular velocity of the motor is changed by changing the duty cycle value of the motor driver, the duty cycle is increased from 5% to 10% with 0.1% increments. The propeller angular velocities are measured with tachometer during these changes to the tachometer. From this experiments, the relationship between the angular velocity and the duty cycle is obtained. The second experiment is conducted to generate the thrust force due to the rotation of the propellers of the Quadrotor by using the following equation:

$$F = b\Omega^{2}$$
(2.1)

where,

F = thrust force (N),

b = thrust factor,

 $\Omega$  is the angular velocity of the propeller (rad/s).

Lastly, this author conducts the bifilar pendulum experiment in order to calculate the moment of inertia of the Quadrotor. This experiment is conducted by hanging the system from two sides with ropes. The whole system is then rotated and released free. The system starts to swing about the axis due to the tension on the ropes which able to lead to the calculation of the inertia. With the help of this experiment, the moment of inertias about the movements of the Quadrotor are able to be determined. Since the system is symmetric, the

mass moment of inertia about roll and pitch axes are all assumed to be the same. The mass moment of inertia about rotation axis is determined using the following formula:

$$I = \left[\frac{T_n}{2\pi}\right] \frac{mgR^2}{L} \tag{2.2}$$

where,

MALAYSIA

I = mass moment of inertia (kg.m<sup>2</sup>),

 $T_n$  = measured swing period (sec),

m = mass of the system (kg),

g = gravitational acceleration (m/s<sup>2</sup>),

R = distance radius (m),

L = length of the ropes used (m).

The researcher used IMU which is located on the Quadrotor to get the angular rotation data and also obtaining the time taken for the period swing.

Junior J. et. al. [23] state that the signals produced from the inertial sensors were sampled at a rate of 200Hz. It is then digitally processed using the method of complementary filter where this method able to use two or more mathematical functions that complement to each other. This has enable itself on giving rise to the term complementary. This filter consists of a low pass filter and a high pass filter. The low pass filter is applied onto the accelerometer as a device to minimize the high frequency noise from engine vibration. On the other hand, the gyro signal produced by the gyroscope is applied with a high pass filter to remove its drift after integration. The cut-off frequency for both of the high pass filter and the low pass filter must be the same in order to maintain a flat response in the frequency range of interest. The authors have used a cut-off frequency about 1 Hz to produce a good quality of low noise with no drift tilt signal.

# 2.3 Summary and Discussion of the Review

In this new era of globalisation which is full with technologies, the Quadrotor is being developed in many ways which is difference in many ways such as the operational function of the model, the types of hardware configuration in terms of the shape of the body frame and also the movement of the model due to the angular velocity of the rotors. Even the method of modelling the mathematical equations are different among each other. The choices of them are being summarized and shown in Table 2.1.

Table 2.1: The summary of each journal

Title	Author	Method of	Body	Experiment	Propeller
Title	Aumor	Modelling	Frame	Conducted	Driver
Control Platform  Design and  Experiment of a  Quadrotor	Jiang J., Qi J.T., Song D.L. & Han J.D.	Newton- Euler formulation	+ shaped	N/A	Brushless DC Motor
Modelling, Simulation and Implementation of a Quadrotor UAV	Fernando, H.C.T.E., De Silva, A.T.A., De Zoysa, M.D.C., Dilshan, K.A.D.C. & Munasinghe, S.R.	Newton- Euler formulation	X- shaped	اونیور N/A IELAKA	Brushless DC Motor
Control of a  Quadrotor Using a  Smart Self-Tuning  Fuzzy PID  Controller	Deepak G. & Cheolkeun H.	Newton- Euler formulation	X- shaped	Observation at low speed of rotor	4 Small motors with no gearbox
Modeling and Simulation of an Autonomous Quad- Rotor Microcopter	Aleksandar R. & Gyula M.	Newton- Euler formulation	+ shaped	Open-loop simulation using MATLAB	Electronic Motor

Quad-Rotor Unmanned Aerial Vehicle Helicopter Modelling & Control	Yogianandh N., Riaan S. & Glen B.	Euler- Lagrange equations	+ shaped	Momentum for Blade and Rotor	N/A
Modelling and Decentralized Adaptive Tracking Control of a Quadrotor UAV	Mostafa M. & Alireza M.	Euler- Lagrange equations	X- shaped	N/A	Brushless DC Motor
Self-tuning PID Control Design for Quadrotor UAV	Yang J. P. Cai Z.H., Qing L. & Wang Y.X.	Euler	X- shaped	Pendulum test method	Electronic Motor
Modeling and Neural Control of Quadrotor Helicopter  "Quadrotor – An Unmanned Aerial Vehicle"	Yasir A. & Valiuddin A.  Shah K. N., Dutt B.  J. & Modh H.	N/A N/A AL	+ shaped + shaped	Determination of Yaw, Roll and Pitch angle, Force and Moment of Inertia of Quadrotor Determination of physical measurement using CREO modelling software	Brushless DC Motor  Brushless DC Motor
Adaptive Control for Quadrotors	Ameho Y., Niel F., Defay F., Biannic J. & Berard C.	Euler's method	X- shaped	Test using two different weight	N/A
Influence of Forward and Descent Flight on Quadrotor Dynamics	Orsag M. & Bogdan S.	Euler's method	X- shaped	Determination the rotation speed, induced speed and the thrust of motor	Standard Brushed DC Motor

Design, Construction and Control of a Large Quadrotor Micro Air Vehicle	Edward P. & Pounds I.	Euler's method	X- shaped	Experimenting the rotor's performance	Brushless DC Motor
Attitude and Altitude Control of an Outdoor Quadrotor	Güçlü A.	Newton- Euler formulation	X- shaped	Force lift, motor speed test and Bifilar Experiment	Brushless DC Motor
Stability Control of a  Quad-Rotor using a  PID Controller	Junior J Paula J., Leandro G. & Bonfim M.	N/A	X- shaped	Complementary Filter	Brushless electric motor
Design of an Integrated Electronic Speed Controller for Compact Robotic Vehicles	Tefay, B., Eizad, B., Crosthwaite, P., Singh, S., & Postula, A.	N/A	N/A	Determination of duty cycle and RPM threshold	Brushless electric motor

The table 2.1 have given a great help on the extraction of ideas for the completion of this project. The methods of choice used to design the mathematical modelling of the hardware and the choice of hardware design of the Quadrotor is shown in Table 2.2 in order to complete the final year project.

Table 2.2: The methods and the hardware configuration for this project

Methods of Modelling	Body Frame Configuration	Quadrotor's movement	Experiments Conducted	Motor Driver
1.) Newton- Euler formulation 2.) SimMechani cs toolbox	X-shaped	Yaw Pitch Roll Vertical	Physical Measurement, Force Lift and Thrust force for Quadrotor	Brushless DC Motor

In overall, the basic principles and the theories are reviewed and synthesized in terms of the functions and the advantage of the usage of it. Nonetheless, the characteristics and the configurations of the Quadrotor are taken into account for developing an accurate mathematical modelling of the hardware before continue on developing the controller for

the Quadrotor. Firstly, Newton-Euler formulation is chosen due to this method will give a better result and more accurate compared with other methods such as Euler-Lagrange. SimMechanics toolbox is used to model using existing functional blocks such as body, joints and many more without the need of mathematical modelling and the most important things needed is the parameter of the variable. The Quadrotor required six degree of freedom to be able to fly. The six degree of freedom consist of 3 axis (x,y,z) accelerometer and 3 axis gyroscope  $(\phi, \theta, \psi)$ . In addition, since the body frame configuration is important for the mathematical modelling, X-shaped of the body frame configuration is chosen rather than + shaped is due to X-shaped body frame is symmetrical and is able to move vertically. In addition, brushless DC motors is used to drive every propeller due to its high efficiency for its high torque per weight and high torque per watt. Finally, the propeller is the main component which enable the movements of the Quadrotor. This Quadrotor uses 4 propellers as the same as other researches where each propeller consists of two blades. The movements of the Quadrotor is chosen which is the yaw, pitch, roll and vertical. Last but not least, the experiments that are chose to be conducted for easing the process of this project is the experiment to obtain the physical measurement of every component used, the force lift and

اونیون سیتی تیکنیک ملیسا ملاك

UNIVERSITI TEKNIKAL MALAYSIA MELAKA

### **CHAPTER 3**

### RESEARCH METHODOLOGY

This chapter is the proposed methodology of the study which are implemented to accomplish this project. Proper planning for this methodology are needed to complete the research which includes the selection of components, the development of model, simulation and analysing the results. According to the studies on the previous research about the characteristics and specifications, the methodology are expected to be most proper methods, techniques and tools in order to accomplish this research.

### 3.1 Project Overview

The main purpose of the methodology is to ensure all the work procedures are in systematic and in an orderly process for accomplishing the objectives according to the whole scopes of study. In addition, the SOP is used as the benchmark for all procedures involving the techniques, methods and testing. Furthermore, these systematic sets of procedures are also based on previous related work. Figure 3.1 shows the flow chart for the overall process in obtaining the final result in order to achieve the objective to clarify the sets of technique and method in this research. This research begins with determining its hardware configuration and defining the components. Then, the development of modelling for Quadrotor is done and is follow by analysing it. The next step is to undergo suitable experiments for determining the input equation for Quadrotor. After that, model the computational mathematical modelling using SimMechanics Toolbox with the help of Solidwork. The derivation of the mathematical modelling is done by using Newton-Euler method. The modelling is then simulated to configure its specific variable. Analysis for both of the modelling is done and thus implementing each of the variables onto the Quadrotor

input equation. The result is being analysed finally. The gantt chart for the overall project is stated in Appendix A.

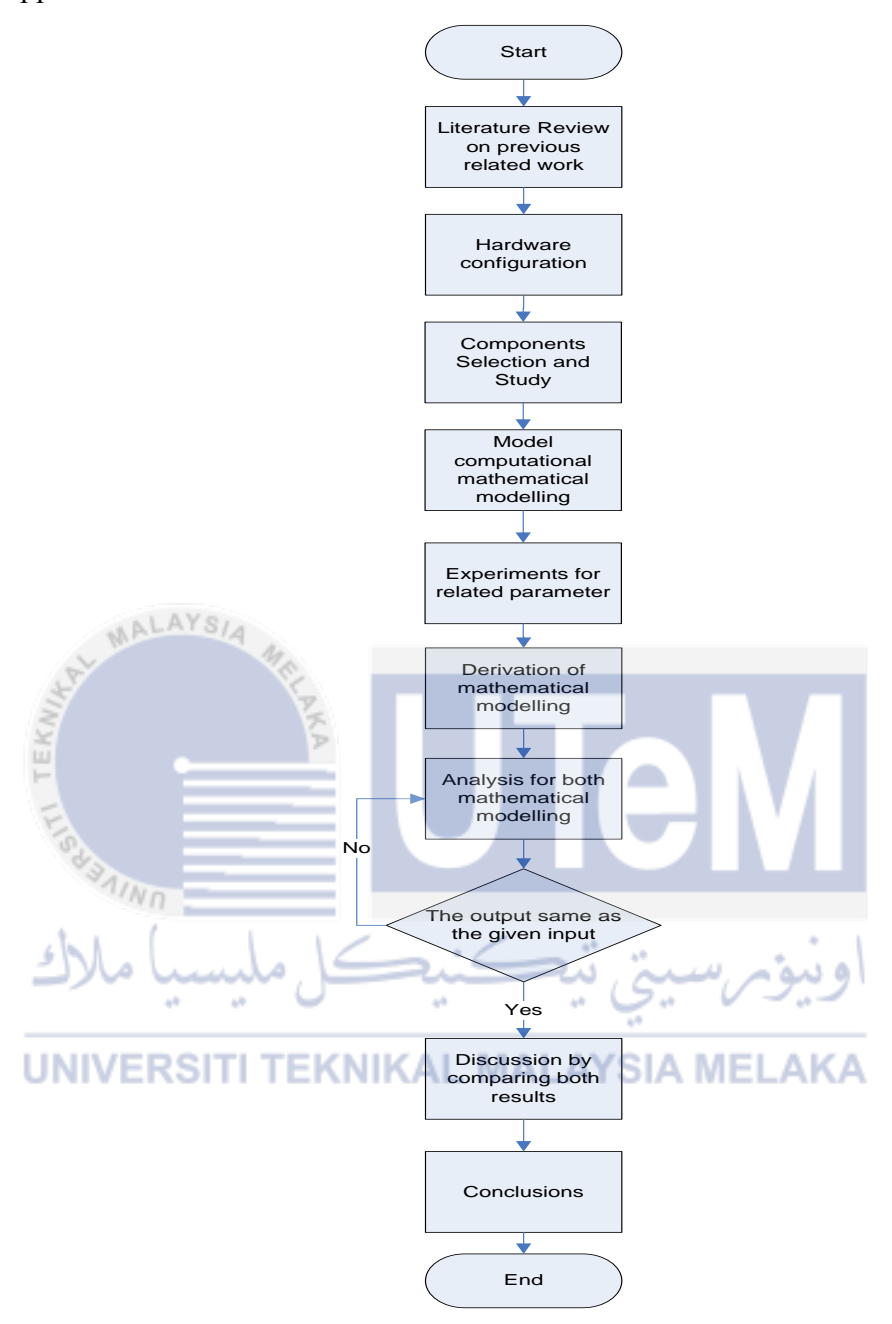


Figure 3.1: Overall project flowchart

### 3.2 Testbed's Components

The selection of the components is very important among the others as all the process of this research are depending on the selected components. The components should be selected based on its performance and specifications which able to give a better result when being assemble together to become a Quadrotor system.

### 3.2.1 **Motor**

Motor used in the Quadrotor system is the Brushless DC motor. To be more specific, it is Turnigy D283011 1000kV brushless motor. Total of four motors is used to drive the propellers with given input signal. It has three different colours of cable where the black wire represents the ground cable, the yellow wire and red wire represents the signal input cable. The cables is connect the electronic speed controller. The direction of the rotation for the motor is depending on the order of connection.



Propellers are used as counter-rotating propellers in the Quadrotor and are mainly for controlling the movement of the Quadrotor. There are four equally and similar propellers used in Quadrotor system. There are two propellers rotating in clockwise direction while the other two propellers rotating in opposite direction. This configuration is due to cancellation of each other's drag force that produced from the propeller in order to stabilize the Quadrotor.

### 3.2.3 Framework

The framework of this Quadrotor is consist of the base of the Quadrotor, the frames of the Quadrotor and the landing gears of the Quadrotor. The most important part of the Quadrotor is the base as it is the main node for the system. It has two base used which is the upper base and the lower base. Both are in square shape. Its function is to hold the frames and all the components together strongly and tightly from separating when the Quadrotor is flying. The spaces in between is filled with the electronic speed controllers and the power distributor cable. Another important part of this Quadrotor is the frame. It acts like the skeletal in a human body. Its configuration represents the shape and size of the Quadrotor. The end portion of the frame is fixed to a motor to drive a propeller while the inner portion is fixed onto the base of the Quadrotor. The weight of the whole system is usually depending on the material used for the frame. There are four similar frames are used where all of it is a square hollow bar. This is used to reduce the weight of the frame and keeping the strength of the frame at the same time. Basically, the landing gear is fixed onto the frame to make sure the Quadrotor is safely landed or a device to decrease the impact force if any accidents occurred as it is free falling onto the ground. This part is quite similar to the frame as the material used is hollow bar in order to reduce the weight but retain its usefulness of the gear.

## 3.2.4 Platform INIVERSITI TEKNIKAL MALAYSIA MELAKA

The platform used in this Quadrotor is Arduino Uno. Arduino is an open-source electronics platform that is based on easy-to-use hardware or software, simple I/O board and development environment that implements the wiring or process language. This kind of Arduino uses ATmega328 microcontroller which has 14 digital I/O pins, where 6 of it are able to provide PWM signals, and 6 analogue inputs that uses 16 MHz of ceramic resonator and contain 32kB of flash memory, a power jack, a reset button, a USB connection and an ISCP header.

### 3.2.5 IMU

IMU is a Inertial Measurement Unit which is an electronic device that is used to give measurements and provide reports typically on the prototype's velocity, orientation and gravitational forces. Normally, IMU used is the accelerometers and gyroscopes. This devices is to collect the angular velocity and acceleration before sending the data to the microcontroller to process it. The IMU used for this research is the ADXL345 accelerometer and the L3G4200D gyroscope. IMU usually comes with 10 degree of freedom but this project only uses 6 degree of freedom that represents the 3 axis of accelerometer and 3 axis of gyroscope. By using these 6 degree of freedom, the orientation and the position of an object in space can easily to be determined.

# 3.3 Derivation of Mathematical Modelling The Quadcopter system that is developed represented in terms of mathematical model as the following. 3.3.1 Dynamic Modelling of Quadrotor

The dynamic modelling of the Quadrotor comprises the state variables equations, the kinematics of the prototype, the dynamics of the rigid body, the moment of inertia for the whole system and the force and moments of the Quadrotor.

### 3.3.2 State Variables of Quadrotor

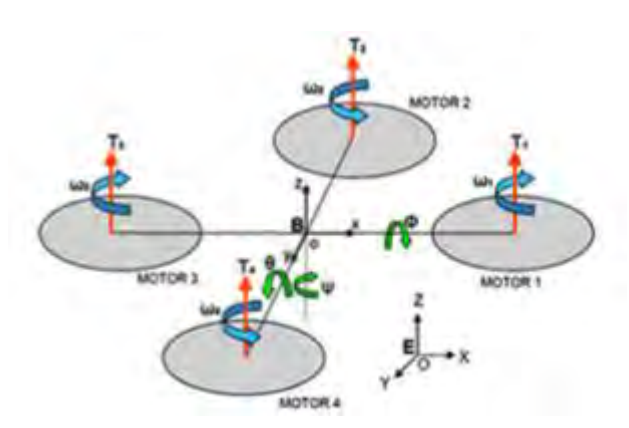


Figure 3.2: Definition of Axes [7]

From the Figure 3.2 as shown above, the state variables of the Quadrotor are based on the Figure above. The body frame is represented by variable b while variable E represents the inertial frame. The position of the three axes (x, y, z) of the Quadrotor is relative to the inertial frame. The rotation about x-axis produces  $\phi$  angle which is the rolling angle, the rotation about y-axis produces  $\theta$  angle which is the pitching angle, and the rotation about z-axis produces  $\varphi$  angle which is the yaw angle. Besides, the translational velocity  $(\dot{x}, \dot{y}, \dot{z})$  and the angular velocity  $(\dot{\varphi}, \dot{\theta}, \dot{\varphi})$  of the Quadrotor are set in relative to the body frame situated in the middle of the Quadrotor.

The modelling of the Quadrotor are being modelled by assuming:

- i. The structure of the Quadrotor is symmetrical and rigid.
- ii. Every each propeller is rigid in plane.
- iii. The centre of mass for the Quadrotor coincides with the origin of body frame of the Quadrotor.
- iv. The inertia matrix is time-invariant.

### 3.3.3 **Kinematics of Quadrotor**

Due to Newton-Euler method, its derivation is due to the rotational movement of the Quadrotor. The following is the relationship between the position and velocities of the Quadrotor. Let b is the base frame and v is the axis of movement, the c represents cosine and s represents sine.

$$\frac{d}{dt} \begin{pmatrix} x \\ y \\ -z \end{pmatrix} = R_b^{\nu} \begin{pmatrix} \ddot{x} \\ \ddot{y} \\ \ddot{z} \end{pmatrix} \tag{3.1}$$

$$= (R_{\nu}^{b})^{T} \begin{pmatrix} \ddot{x} \\ \ddot{y} \\ \ddot{z} \end{pmatrix} \tag{3.2}$$

$$= \begin{pmatrix} c\theta c\varphi & s\varphi s\theta s\varphi - c\varphi s\varphi & c\varphi s\theta c\varphi + s\varphi s\varphi \\ c\theta s\varphi & s\varphi s\theta s\varphi + c\varphi s\varphi & c\varphi s\theta c\varphi - s\varphi s\varphi \\ -s\theta & c\theta s\varphi & c\theta c\varphi \end{pmatrix} \begin{pmatrix} \ddot{x} \\ \ddot{y} \\ \ddot{z} \end{pmatrix}$$
(3.3)

The relationship between  $\dot{\phi}$ ,  $\dot{\theta}$ ,  $\dot{\phi}$  and  $\ddot{\phi}$ ,  $\ddot{\theta}$ ,  $\ddot{\varphi}$  is:

$$R_{v2}^{b}(\dot{\phi}) = R_{v1}^{v2}(\dot{\dot{\phi}}) = R_{v}^{v1}(\dot{\phi}) = I$$
This leads to:
$$(3.4)$$

$$\begin{pmatrix} \ddot{\boldsymbol{\varphi}} \\ \ddot{\boldsymbol{\theta}} \\ \boldsymbol{\varphi} \end{pmatrix} = R_{v2}^{b} (\dot{\boldsymbol{\varphi}}) \begin{pmatrix} \dot{\boldsymbol{\varphi}} \\ 0 \\ 0 \end{pmatrix} + R_{v1}^{v2} (\dot{\boldsymbol{\theta}}) \begin{pmatrix} 0 \\ \dot{\boldsymbol{\theta}} \\ 0 \end{pmatrix} + R_{v}^{v1} (\dot{\boldsymbol{\varphi}}) \begin{pmatrix} 0 \\ 0 \\ \dot{\boldsymbol{\varphi}} \end{pmatrix}$$
(3.5)

$$= \begin{pmatrix} \dot{\phi} \\ 0 \\ 0 \end{pmatrix} + \begin{pmatrix} 1 & 0 & 0 \\ 0 & c\phi & s\phi \\ 0 & -s\phi & c\phi \end{pmatrix} \begin{pmatrix} 0 \\ \dot{\theta} \\ 0 \end{pmatrix} + \begin{pmatrix} 1 & 0 & 0 \\ 0 & c\phi & s\phi \\ 0 & -s\phi & c \end{pmatrix} \begin{pmatrix} c\theta & 0 & -s\theta \\ 0 & 1 & 0 \\ s\theta & 0 & c\theta \end{pmatrix} \begin{pmatrix} 0 \\ 0 \\ \dot{\phi} \end{pmatrix}$$
(3.6)

$$\begin{pmatrix} \ddot{\phi} \\ \ddot{\theta} \\ \varphi \end{pmatrix} = \begin{pmatrix} 1 & 0 & 0 \\ 0 & c\phi & s\phi \\ 0 & -s\phi & c\phi \end{pmatrix} \begin{pmatrix} \dot{\phi} \\ \dot{\theta} \\ \dot{\varphi} \end{pmatrix} \tag{3.7}$$

By inverting the equation 4,

$$\begin{pmatrix} \dot{\phi} \\ \dot{\theta} \\ \dot{\varphi} \end{pmatrix} = \begin{pmatrix} 1 & s\phi \tan\theta & c\phi \tan\theta \\ 0 & c\phi & -s\phi \\ 0 & s\phi \sec\theta & c\phi \sec\theta \end{pmatrix} \begin{pmatrix} \ddot{\phi} \\ \ddot{\theta} \\ \varphi \end{pmatrix}$$
 (3.8)

### 3.3.4 Dynamics of Rigid Body

Now, let variable **v** represents the velocity vector of the Quadrotor. Thus, the translational motion of the Quadrotor is as follows:

$$f = ma ag{3.9}$$

$$f = m \frac{dv}{dt} \tag{3.10}$$

$$f = m\left(\frac{d\mathbf{v}}{dt_b} + \omega_{b/i} \times \mathbf{v}\right) \tag{3.11}$$

Where  $\omega_{b/i}$  is the angular velocity of the base frame, b, with relative to the inertial frame, i. Expressing the equation 3 in body coordinates format becomes:

$$\begin{pmatrix} \dot{\mathbf{u}} \\ \dot{v} \\ \dot{w} \end{pmatrix} = \begin{pmatrix} \ddot{\varphi}\ddot{y} - \ddot{\theta}w \\ \ddot{\varphi}\ddot{w} - \ddot{\varphi}x \\ \ddot{\theta}\ddot{y} - \ddot{\varphi}y \end{pmatrix} + \frac{1}{m} \begin{pmatrix} f_x \\ f_y \\ f_z \end{pmatrix}$$
 (3.12)

Given that the rotational matrix that related to mass, m, is:

$$\boldsymbol{m} = \frac{d\mathbf{z}}{dt_i} = \frac{d\mathbf{z}}{dz_b} + \omega_{b/i} \times \mathbf{z} \tag{3.13}$$

Thus, the constant inertia matrix, I, can be able to deduce:

$$I = \begin{pmatrix} \int (y^{2} + z^{2})dm & -\int xy \, dm & -\int xz \, dm \\ -\int xy \, dm & \int (x^{2} + z^{2})dm & -\int yz \, dm \\ -\int xz \, dm & -\int yz \, dm & \int (x^{2} + y^{2})dm \end{pmatrix}$$
(3.14)

$$\triangleq \begin{pmatrix} I_{x} & -I_{xy} & -I_{xz} \\ -I_{xy} & I_{y} & -I_{yx} \\ -I_{xz} & -I_{yz} & I_{z} \end{pmatrix}$$
(3.15)

### 3.3.5 Moment of Inertia of Quadrotor

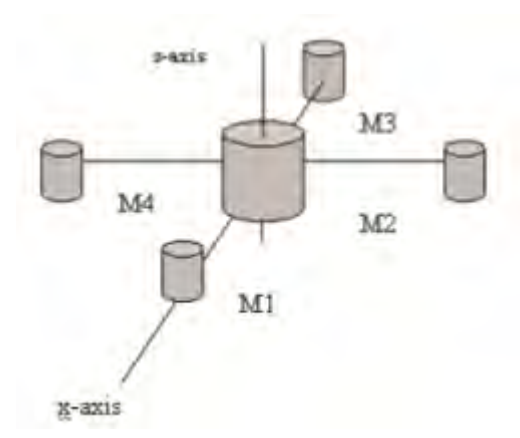


Figure 3.3: An assumption of a Quadrotor shape for derivation of inertia [6]

The Figure 3.3 shown above is an assumed shape for the inertia of the Quadrotor where the M represents respective motor while the cylinder in the centre has a mass, m, and radius, R. A Quadrotor that is assumed to be symmetrical about all three axes which will give results as follows:

The inverse of *I* is as follows:

$$I^{-1} = \begin{pmatrix} \frac{1}{I_x} & 0 & 0 \\ 0 & \frac{1}{I_y} & 0 \\ 0 & 0 & \frac{1}{I_z} \end{pmatrix}$$
 (3.17)

where the equation of inertia for the 3 axes (x, y and z) is denoted as:

$$I_{x/y} = \frac{2MR^2}{5} + 2l^2m \tag{3.18}$$

$$I_{z=} \frac{2MR^2}{5} + 4l^2m \tag{3.19}$$

By defining  $m^b = (\tau_{\phi}\tau_{\theta}\tau_{\varphi})^T$ , we are able to write the related equation (2) in body coordinates form which is:

$$\begin{pmatrix} \ddot{\boldsymbol{\phi}} \\ \ddot{\boldsymbol{\theta}} \\ \ddot{\boldsymbol{\varphi}} \end{pmatrix} = \begin{pmatrix} \frac{1}{I_x} & 0 & 0 \\ 0 & \frac{1}{I_y} & 0 \\ 0 & 0 & \frac{1}{I_z} \end{pmatrix} \begin{bmatrix} \begin{pmatrix} 0 & \ddot{\boldsymbol{\varphi}} & \ddot{\boldsymbol{\theta}} \\ \ddot{\boldsymbol{\varphi}} & 0 & \ddot{\boldsymbol{\varphi}} \\ \ddot{\boldsymbol{\theta}} & \ddot{\boldsymbol{\varphi}} & 0 \end{pmatrix} \begin{pmatrix} J_x & 0 & 0 \\ 0 & J_y & 0 \\ 0 & 0 & J_z \end{pmatrix} \begin{pmatrix} \ddot{\boldsymbol{\varphi}} \\ \ddot{\boldsymbol{\theta}} \\ \boldsymbol{\varphi} \end{pmatrix} + \begin{pmatrix} \tau_{\boldsymbol{\varphi}} \\ \tau_{\boldsymbol{\varphi}} \\ \tau_{\boldsymbol{\varphi}} \end{pmatrix} \end{bmatrix}$$
(3.20)

$$= \begin{pmatrix} \frac{I_{y} - I_{z}}{I_{x}} \ddot{\theta} \ddot{\varphi} & 0 & 0 \\ 0 & \frac{I_{z} - I_{x}}{I_{y}} \ddot{\varphi} \ddot{\varphi} & 0 \\ 0 & 0 & \frac{I_{x} - I_{y}}{I_{z}} \ddot{\varphi} \ddot{\theta} \end{pmatrix} + \begin{pmatrix} \frac{1}{I_{x}} \tau_{\varphi} \\ \frac{1}{I_{y}} \tau_{\theta} \\ \frac{1}{I_{z}} \tau_{\varphi} \end{pmatrix}$$
(3.21)

6 degree of freedom model for the kinematics and dynamics of Quadrotor can be summarized as follows:

$$\begin{pmatrix} \dot{x} \\ \dot{y} \\ \dot{z} \end{pmatrix} = \begin{pmatrix} c\theta c\varphi & s\varphi s\theta s\varphi - c\varphi s\varphi & c\varphi s\theta c\varphi + s\varphi s\varphi \\ c\theta s\varphi & s\varphi s\theta s\varphi + c\varphi s\varphi & c\varphi s\theta c\varphi - s\varphi s\varphi \\ -s\theta & c\theta s\varphi & c\theta c\varphi \end{pmatrix} \begin{pmatrix} \ddot{x} \\ \ddot{y} \\ \ddot{z} \end{pmatrix}$$
 (3.22)

$$\begin{pmatrix} \ddot{x} \\ \ddot{y} \\ \ddot{z} \end{pmatrix} = \begin{pmatrix} \ddot{\varphi}\ddot{y} - \ddot{\theta}\ddot{z} \\ \ddot{\varphi}\ddot{z} - \ddot{\varphi}\ddot{x} \\ \ddot{\varphi}\ddot{x} - \ddot{\varphi}\ddot{y} \end{pmatrix} + \frac{1}{m} \begin{pmatrix} f_x \\ f_y \\ f_z \end{pmatrix}$$
 (3.23)

$$\begin{pmatrix} \dot{\phi} \\ \dot{\theta} \\ \dot{\varphi} \end{pmatrix} = \begin{pmatrix} 1 & s\phi \tan\theta & c\phi \tan\theta \\ 0 & c\phi & -s\phi \\ 0 & \frac{s\phi}{c\theta} & \frac{c\phi}{c\theta} \end{pmatrix} \begin{pmatrix} \ddot{\phi} \\ \ddot{\theta} \\ \varphi \end{pmatrix}$$
 (3.24)

$$\begin{pmatrix} \ddot{\Theta} \\ \ddot{\theta} \\ \ddot{\varphi} \end{pmatrix} = \begin{pmatrix} \frac{I_{y} - I_{z}}{I_{x}} \ddot{\Theta} \ddot{\varphi} \\ \frac{I_{z} - I_{y}}{I_{y}} \ddot{\Theta} \ddot{\varphi} \\ \frac{I_{x} - I_{y}}{I_{z}} \ddot{\Theta} \ddot{\theta} \end{pmatrix} + \begin{pmatrix} \frac{1}{I_{x}} \tau_{\Phi} \\ \frac{1}{I_{y}} \tau_{\theta} \\ \frac{1}{I_{z}} \tau_{\varphi} \end{pmatrix}$$
(3.25)

### 3.3.6 Force and Moments

The force and the moments are typically due to the gravitational force and the four propellers which is located on every motor.

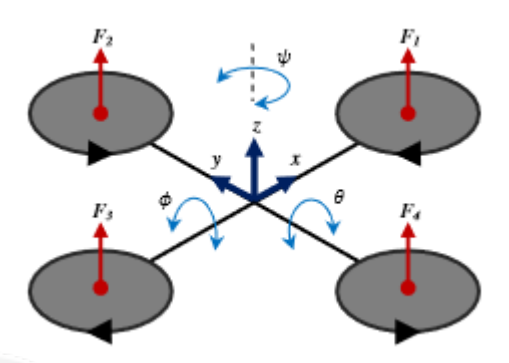


Figure 3.4: The definition of forces and torques acting on the motors of the Quadrotor [23]

Total force acting on the Quadrotor as follows:

$$F = F_f + F_r + F_b + F_l (3.26)$$

Formula of torque for pitching as follows:

$$\tau_{\theta} = l(F_f - F_b) \tag{3.27}$$

Formula of torque for rolling as follows:

$$\tau_{\Phi} = l(F_l - F_r) \tag{3.28}$$

Formula of torque for total yawing as follows:

$$\tau_{\varphi} = \tau_r - \tau_l - \tau_f - \tau_b \tag{3.29}$$

Calculation for force of each motor as follows:

$$F_* = k_1 \delta_* \tag{3.30}$$

Calculation for torque of each motor as follows:

$$\tau_* = k_2 \delta_* \tag{3.31}$$

Derivation of matrix form of force and torques of Quadrotor

$$\begin{pmatrix} F \\ \tau_{\phi} \\ \tau_{\theta} \\ \tau_{\varphi} \end{pmatrix} = \begin{pmatrix} k_1 & k_1 & k_1 & k_1 \\ 0 & -lk_1 & 0 & lk_1 \\ lk_1 & 0 & lk_1 & 0 \\ -k_2 & k_2 & -k_2 & k_2 \end{pmatrix} \begin{pmatrix} \delta_f \\ \delta_r \\ \delta_b \\ \delta_l \end{pmatrix} \triangleq M \begin{pmatrix} \delta_f \\ \delta_r \\ \delta_b \\ \delta_l \end{pmatrix}$$

$$(3.32)$$

Convert equation into body frame as follows:

$$F_g^b = R_v^b \begin{pmatrix} 0 \\ 0 \\ mg \end{pmatrix} = \begin{pmatrix} -mg \ s\theta \\ mg \ c\theta s\theta \\ mg \ c\theta c\Phi \end{pmatrix}$$
(3.33)

Therefore, from the above equations, the twelve equation of motion of a Quadrotor are derive and as follows:

$$\begin{pmatrix} \dot{x} \\ \dot{y} \\ \dot{z} \end{pmatrix} = \begin{pmatrix} c\theta c\varphi & s\varphi s\theta s\varphi - c\varphi s\varphi & c\varphi s\theta c\varphi + s\varphi s\varphi \\ c\theta s\varphi & s\varphi s\theta s\varphi + c\varphi s\varphi & c\varphi s\theta c\varphi - s\varphi s\varphi \\ -s\theta & c\theta s\varphi & c\theta c\varphi \end{pmatrix} \begin{pmatrix} \ddot{x} \\ \ddot{y} \\ \ddot{z} \end{pmatrix}$$
 (3.34)

$$\begin{pmatrix} \ddot{x} \\ \ddot{y} \\ \ddot{z} \end{pmatrix} = \begin{pmatrix} \ddot{\varphi}\ddot{y} - \ddot{\theta}\ddot{z} \\ \ddot{\varphi}\ddot{z} - \ddot{\varphi}\ddot{x} \\ \ddot{\varphi}\ddot{x} - \ddot{\varphi}\ddot{y} \end{pmatrix} + \begin{pmatrix} -g \ s\theta \\ g \ c\theta s\theta \\ g \ c\theta c\phi \end{pmatrix} + \frac{1}{m} \begin{pmatrix} 0 \\ 0 \\ - \ddot{F} \end{pmatrix}$$
 (3.35)

$$\begin{pmatrix} \dot{\phi} \\ \dot{\theta} \\ \dot{\phi} \end{pmatrix} = \begin{pmatrix} 1 & s\phi \tan\theta & c\phi \tan\theta \\ 0 & c\phi & -s\phi \\ 0 & \frac{s\phi}{c\theta} & \frac{c\phi}{c\theta} \end{pmatrix} \begin{pmatrix} \ddot{\phi} \\ \ddot{\theta} \\ \varphi \end{pmatrix}$$
 (3.36)

$$\begin{pmatrix} \ddot{\Theta} \\ \ddot{\theta} \\ \ddot{\varphi} \end{pmatrix} = \begin{pmatrix} \frac{I_{y} - I_{z}}{I_{x}} \ddot{\Theta} \ddot{\varphi} \\ \frac{I_{z} - I_{y}}{I_{y}} \ddot{\Theta} \ddot{\varphi} \\ \frac{I_{x} - I_{y}}{I_{z}} \ddot{\Theta} \ddot{\theta} \end{pmatrix} + \begin{pmatrix} \frac{1}{I_{x}} \tau_{\Phi} \\ \frac{1}{I_{y}} \tau_{\theta} \\ \frac{1}{I_{z}} \tau_{\varphi} \end{pmatrix}$$
(3.37)

Hence, the simplified equations of the motion of Quadrotor are given by:

$$\ddot{x} = (-c\phi s\theta c\varphi - s\phi s\varphi)\frac{F}{m} \tag{3.38}$$

$$\ddot{y} = (-c\phi s\theta c\varphi + s\phi c\varphi)\frac{F}{m} \tag{3.39}$$

$$\ddot{z} = g - (c\phi c\theta) \frac{F}{m} \tag{3.40}$$

$$\ddot{\Phi} = \frac{1}{I_r} \tau_{\Phi} \tag{3.41}$$

$$\ddot{\theta} = \frac{1}{I_y} \tau_{\theta} \tag{3.42}$$

$$\ddot{\varphi} = \frac{1}{I_z} \tau_{\varphi} \tag{3.43}$$

The input equation to the Quadrotor are given by:

MALAYSIA

$$u_{roll} = lb(-\omega_2^2 + \omega_4^2) \tag{3.44}$$

$$u_{pitch} = lb(-\omega_1^2 + \omega_3^2) \tag{3.45}$$

$$u_{yaw} = d(-\omega_1^2 - \omega_3^2 + \omega_2^2 + \omega_4^2)$$
(3.46)

$$u_{throttle} = lb(\omega_1^2 + \omega_2^2 + \omega_3^2 + \omega_4^2)$$
 (3.47)

Finally, the state-space representation of the Quadrotor as follows:

where  $u_1$  is  $u_{throttle}$ ,  $u_2$  is  $u_{roll}$ ,  $u_3$  is  $u_{pitch}$  and  $u_4$  is  $u_{yaw}$ .

### 3.4 Computational Modelling

Computer science to understand and study the behaviour of a complex system or a nonlinear system through the help of computer simulation. Computational modelling requires numerous variables that characterized the Quadrotor system. The simulation with the model is done by just adjusting the parameters of the Quadrotor in the computer and simulate the model in order to study the outcome of the simulation. Besides, this modelling does not require any derivation of any mathematical analytical solution to understand the behaviour of the Quadrotor system. Solidworks software and MATLAB SimMechanics Toolbox are used with the help of SimMechanics Link add-on to model the Quadrotor system. The flowchart below shows the process for this computational modelling of Quadrotor. Figure 3.5 shows the flow for this computational modelling to achieve the first objective.



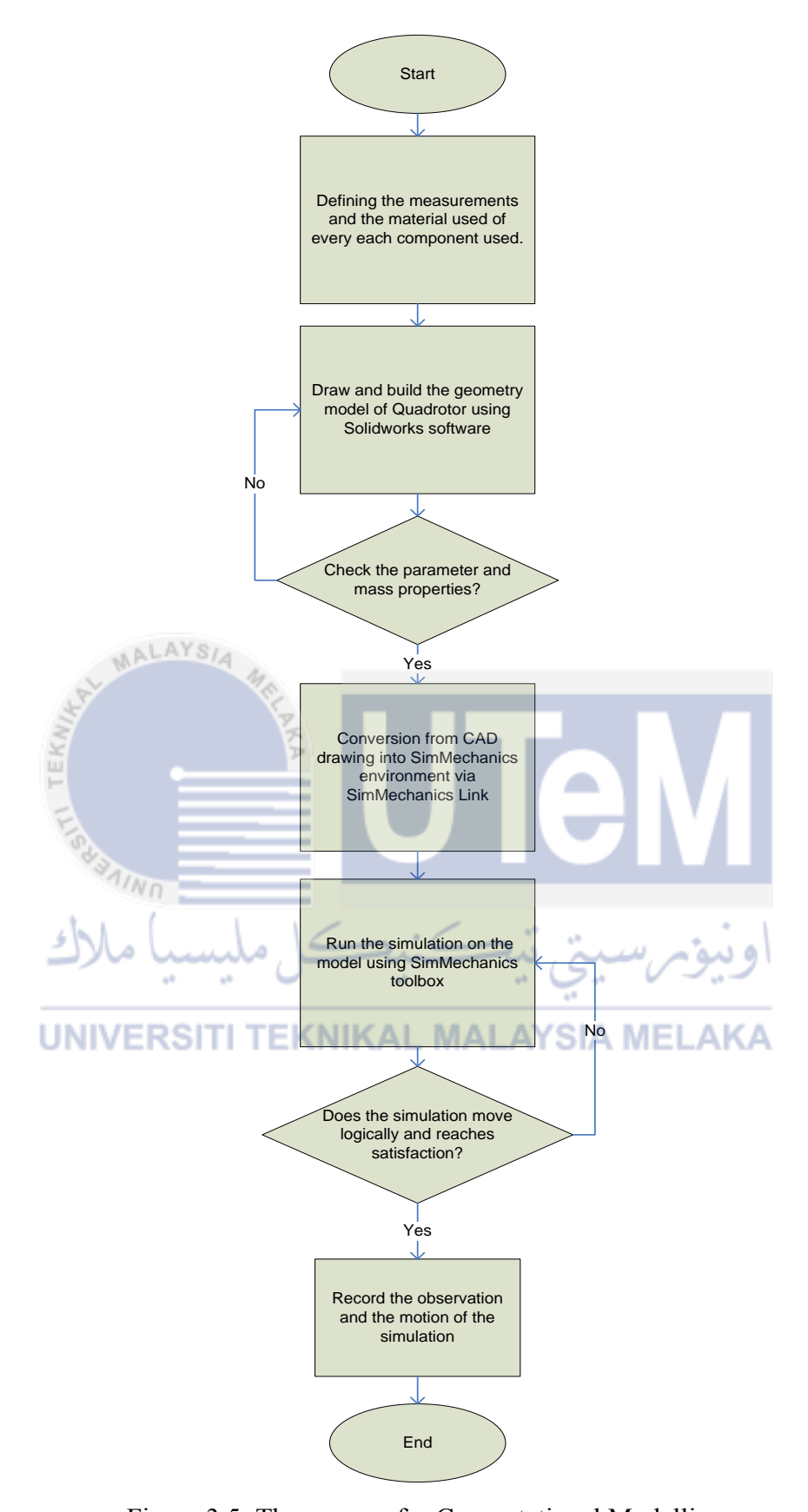


Figure 3.5: The process for Computational Modelling

### 3.4.1 Solidworks

Computer-Aided Design (CAD) is used to assist, modification and making analysis with the use of computer systems such as Solidworks. Thus, this software is used for the process of building models of components used and the evaluation the components' properties through CAD drawing. The flow of using the Solidworks is as the following:-

- i. Study and understand the component to be drawn
- ii. Measure the component in terms of the related length
- iii. Identify the material used on the component
- iv. Sketch the 2D part of the component either in top, front or right plane by following the measurements of the component
- v. Build the 3D part of the component from the 2D drawing using Extruded Boss/Base tools
- vi. Edit or use Extruded Cut tools to take off any unwanted parts of the component drawn
- vii. Evaluate the model for its mass properties such as the centre of mass, the moment of inertia of the model and other properties of the respective model
- viii. Repeat step a. to step g. for other components of the Quadrotor
  - ix. After drawing every each component, assemble all the components together by mating them together depending on which type of the mate is used.
  - x. Record down the mass properties of the whole assemble which represent the system of the Quadrotor.

### 3.4.2 SimMechanics Link

After drawing the CAD of the assembly of the Quadrotor in the Solidworks software environment, this add-on is used to convert the CAD drawing from Solidworks software into SimMechanics model where the parameter and the properties of the parts are also being exported. The flow of using this add-on is as the following:-

- i. Install the add-on and implement onto Solidworks software.
- ii. Open the CAD drawing which is going to be exported. Go to the top bar to press onto "SimMechanics Link" and choose Second generation.

- iii. It will pop-out save screen to save the CAD drawing. This saving will create a XML format file together with .STL format file. STL file carries the geometry model of the CAD drawing.
- iv. Then, go to MATLAB environment and use the smimport command for SimMechanics Second generation or mech\_import command and it is followed by the name of the file to import the CAD drawing.
- v. The CAD drawing is then imported onto Simulink environment.

### 3.4.3 SimMechanics Toolbox

After converting the CAD drawing into SimMechanics Simulink environment via SimMechanics Link add-on, there might be some changes needed to be made on the modelling imported on the Simulink environment due to the limitations of the SimMechanics Links add-on. There are some parts needed to be checked such as the gravitational force, every joints between the bodies and some other important parts. The flow for using this toolbox is as the following and is plotted into a flowchart shown in Figure 3.6:-

- Understand each and every functional blocks which is being imported from the CAD drawing.
- ii. Check whether the parameter and the properties of the model is being imported.
- iii. Check whether the joint and bodies is being mapped following the real Quadrotor.
- iv. Understand the imported model and try running the simulation before editing the model. From this simulation, find the error if any and edit by adding the blocks of changing the parameter within the blocks.
- v. After editing, simulate the model and record the observation on the motion of the model.

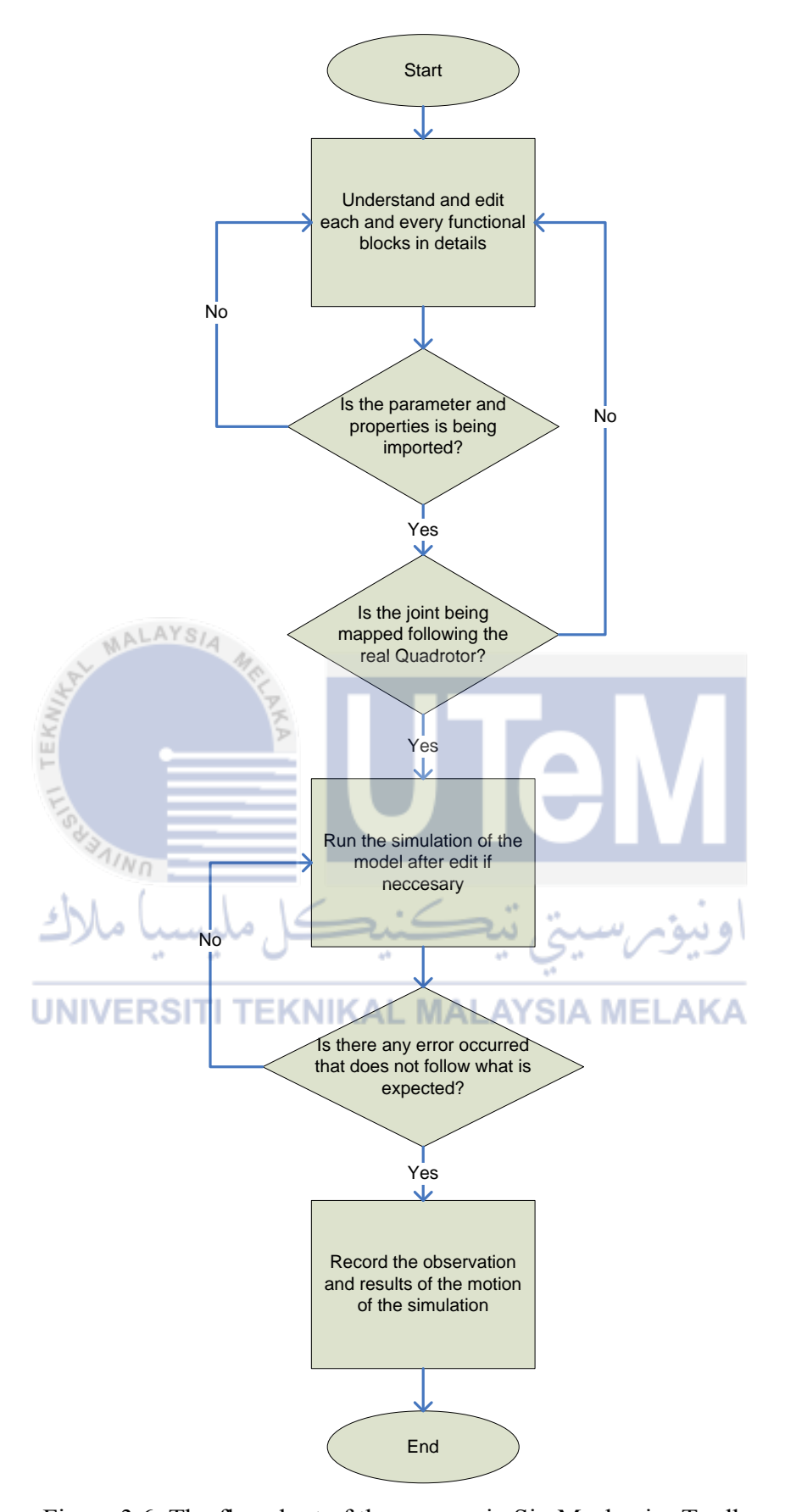


Figure 3.6: The flowchart of the process in SimMechanics Toolbox

### 3.5 Experiments Conducted

There are total of four experiments to be carried out throughout this research in order to determine the input unknown parameters of the Quadrotor system. The experiments that are conducted are the physical measurement, force-lift and rotor's speed test, bifilar experiment and complementary filter.

### 3.5.1 Physical Measurements

In order to obtain a suitable moment of inertia, the parameters of the physical measurement is needed to be measured. Thus, the purpose of conducting this experiment is to obtain the physical measurements of the Quadrotor testbed. There are some parts of the developed Quadrotor testbed can be measured and calculated directly from the testbed itself. The equipment used for this experiment is metre rule and a digital weighing scale machine. Firstly, the overall system of the Quadrotor system and its component is being identified. The size and parameters in terms of length, depth and height of every each components and the overall Quadrotor system are measured using a metre rule. The weight of the whole Quadrotor system and each components are measured using a digital weighing scale. The measurements are repeated for three times for its average measurements. The material of every each components are identified at the moment. Every each related data is recorded together with its unit. The precaution that should be taken into account during the experiment is that parallel error should be avoided while taking reading of measurements when using a metre rule on measuring the parameters of the components to ensure an accurate data measurement. Besides, ensure the zero error on the digital weighing scale machine is correct before taking any measurement to ensure an accurate measurement. Lastly, the precaution should be enforced is to ensure the recorded data are all in the same unit which is the SI units. On the other hand, the reliability for this experiment is that the metre rule and the digital weighing scale machine used should be the same throughout the whole experiment on the measurement of the parameters of the components and the Quadrotor system. Besides, the reliability of this experiments to ensure that the components are to be measured are located in the middle of the weighing surface in order to obtain an accurate measurement.

### 3.5.2 Force-lift and Rotor's Speed Test

The thrust force and the drag force is an important parameter needed to be obtained to find out the input equation into Quadrotor system. Hence, the aim of this experiment is to calculate the value of the thrust factor, b and the drag factor, d by using the force generated by each of the propeller with a given motor speed. A digital weighing scale machine is used to weigh the weight that a propeller that is able to give. From that weight measured, the force of the propeller can be determined. At the same time, a tachometer is used to measure the angular speed of the propeller. It is located perpendicular to the propeller to able to measure the angular speed of the propeller accurately. The Electronic speed controller is used to control the speed of the rotor from given signal by Arduino. The equipment needed for this experiment are the digital weighing scale machine, tachometer, Arduino board and electronic speed controllers (ESC). Firstly, the testbed of the Quadrotor system is placed on the top of the weighing scale machine and the 'zero tare' button is pressed to remove the weight of the equipment. The cable of connection between the motor and the Arduino is place properly. Then, the motor is fixed on top of the holder by using screws and the motor holder is placed on a digital weighing scale machine. The propeller to be experimented is installed upsidedown on the motor. After that, the motor is connected to the ESC that is set to provide anticlockwise rotation with the period of ESC is fixed with 2ms high signal and 1ms low signal. Before the testing, the weightage is set to zero value with the 'zero tare' button pressed. A PWM signal is given to the motor to speed from 40 to 140 with an increment of 10. The measurement value of the digital weightage and the angular speed of the propeller is recorded for every increment. The weight measured by the weighing scale machine is converted onto force by using Newton's Second law to obtain the force-lift generated by the propeller based on the below formula:

$$F = mg (N)$$
where, m = mass measured (kg)
$$g = gravitational force (m/s2)$$

The measurements of the weight and speed is taken for three times and the average is calculated. The steps previously from the start till the end are repeated for testing of the other

three motors. Finally, all the obtained values included the calculated values is recorded in a table.

The precautionary steps are taken into account throughout the process of the experiment by ensuring the 'zero tare' button is pressed before beginning the experiment to avoid any confusion on taking measurement after the experiment. Then, ensure the propeller and the base is screwed tightly and properly as it might be loosen when running the motor and causes injuries while the motor is fixed properly without contacting anything to prevent any short circuit from happening. Finally, the precautionary step should be taken by ensure the motor holder and the weighing scale machine is fixed together to avoid the holder from going off.

On the other hand, the reliability of this experiment is that ensure the battery is fully charge after experimenting with one motor and before proceeding the next attempt on the other motor. Besides, the settings for the Arduino is the same throughout all the experiments on all four motors. The propeller used should be the same for all the experiments on all four motors while a different ESC is used for every each motor for experiment. Last but not least, ensure the scale is zero before beginning the experiment and does not affect the reading during the process of experiment.

# 3.5.3 Bifilar Pendulum Experiment

Moment of inertia of a system is important in order to obtain the equation of the motion of a system. The objective for this experiment is to determine the moment of inertia of the Quadrotor system with the help of the results generated from the physical measurement experiment. In this experiment, the moment of inertia for the Quadrotor to roll, pitch and yaw is measured. A test bench is being constructed in or to carry out this experiment smoothly. The sketching of the test bench is shown in Appendix B. The equipment needed to accomplish this experiment are the test bench which is shown in Appendix B, string, stopwatch, digital weighing scale machine and a metre rule. The procedure for this experiment started by hanging both side of the Quadrotor using string and it is hanged to the test bench. The length of the string from the test bench to the Quadrotor

and the radius of the Quadrotor is measured and recorded for calculation. Then, the testbed is rotated along the z-axis using hand and is released freely for it to rotate by itself. The moment the testbed is released freely, the time on the stopwatch is started until the testbed stop swinging. The time taken on the stopwatch is recorded. The steps from the beginning till the step of recorded the time taken are repeated for three time in order to get an average measurement. The mass moment of inertia of the rotation about the axis is calculated based on the formula:-

$$I = \left[\frac{T_n}{2\pi}\right] \frac{mgR^2}{L} (kgm^2/s)$$

where,  $I = mass moment of inertia (kg.m^2),$   $T_n = measured swing period (sec),$  m = mass of the system (kg),  $g = gravitational acceleration (m/s^2),$  R = distance radius (m),

L = length of the ropes used (m).

The angular rotation data of the testbed is measured using IMU sensor. The data are recorded, presented into a table and plotted into graph to show its relationship. Besides, the mass of each rotor is weighed by using a weighing scale machine. The length of the lever from the motor to the centre of the Quadrotor is measured using a metre rule. Furthermore, the inertial acting reference to the three axis (x, y, z) is determined using the formula:

$$I_x = I_y = \frac{2MR^2}{5} + 2l^2 \overline{m} \qquad \text{(kgm}^2\text{)}$$

$$I_z = \frac{2MR^2}{5} + 4l^2 \overline{m} \qquad \text{(kgm}^2\text{)}$$
where,  $M = \text{mass (kg)}$ 

$$R = \text{Radius distance (m)}$$

$$l = \text{length of the lever (m)}$$

$$\overline{m} = \text{Mass of the respective rotor (kg)}$$

The calculation steps are repeated three time and the average value is recorded.

The precautionary steps are taken into account throughout the process of this bifilar experiment which is avoiding the parallel error while reading the measurement on the metre rule. Besides, the same digital weighing scale machine should be used throughout the whole experiment on the measurement of the weight and ensure the components are to be measured are located in the middle of the weighing surface in order to obtain an accurate measurement. Last but not least, two strings should be ensured that they are tied vertically on the Quadrotor are the same length and tied parallel to each other.

On the other hand, the reliability of bifilar experiment is to conduct the experiments in an indoor area in order to neglect the surroundings and does not affect the measurement value. Besides, the same type of string should be used throughout the whole experiment.

### 3.6 Analysis of Modelling

This part is provides the procedure to analyse the modelling produced based on the computational modelling and the physical modelling. The values or data that is recorded from the computational modelling and physical modelling is used for substituting into the input equation, motion equation and state space representation. Both of the state space representation that is built using computational modelling and physical modelling that represents the system of the Quadrotor. The substituted representation is then changed to differential equation form for analysis. The equation is simulated using MATLAB software with a given input to ensure the desired output is produced. Both of the result is compared in terms of steady state error to compare which modelling used is better and accurate in order to be able to produce a better controller.

### **CHAPTER 4**

### **RESULTS**

### 4.1 Introduction

This chapter provides the results which is used for achieving the objectives which is to computationally and physically model the Quadrotor system using softwares and conducting experiments.

### 4.2 Results of Computational Modelling

This part contains the assembly of the mechanical part of the testbed and the results which is the thrust force of each propeller and the moment of inertia for the testbed. The result is recorded computationally and it is measured with the help of software such as Solidworks and SimMechanics Toolbox.

### 4.2.1 Assembly of Testbed

Figure 4.1 shows the mechanical part of the Quadrotor which is without the on-board system.



Figure 4.1: The assembly of the Quadrotor

The list of components to build the model shown in Figure 4.1 are as follows:

Table 4.1: List of components used in Testbed

Y. Mr.	14010	11. Dist of compone	ints asca in Testeca	•
KNIA	No.	Components	Quantity	
TI TE	1	Base	2	
LISTANINO	2	Frame	4	4
ا ملاك	3	Motor	سىڭ تىد	اونيق
 UNIVER	4 SITI 1	Landing gear	ALAYSIA MEI	 AKA
	5	Propeller	4	
	6	Head-Cap	4	
		Propeller		
	7	Screw bottom	4	
	/	part propeller	+	

Every component used to model the assembly of the Quadrotor is determined and measured computationally using the tools in Solidworks CAD design software. The components are measured and shown in Appendix C.

# 4.2.2 The Block Diagram

After the conversion from the CAD design via SimMechanics Link, the block diagram on the SimMechanics toolbox is produced. The block diagram and the simulation is shown in Figure 4.2.

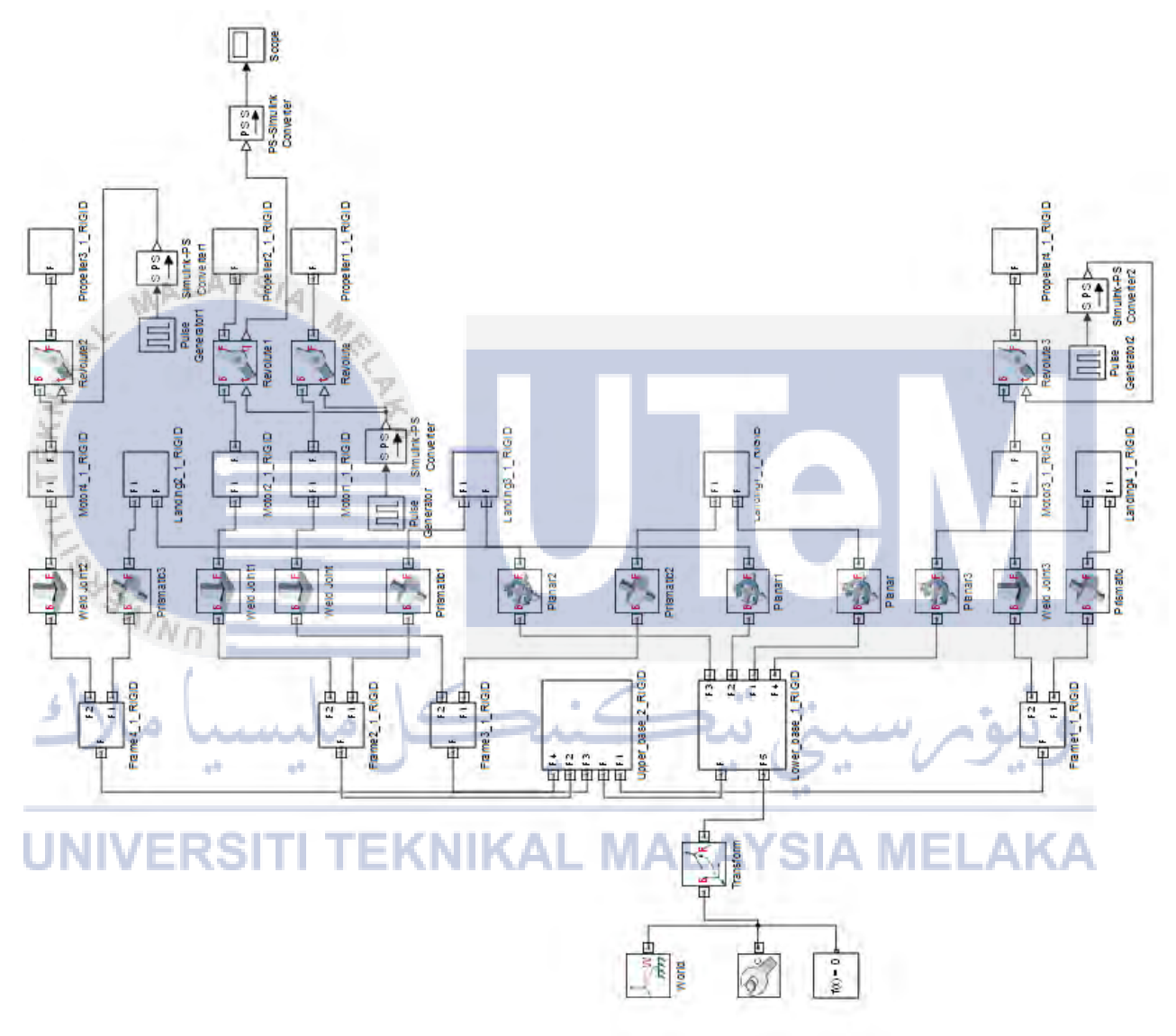


Figure 4.2: The block diagram after the conversion from Solidwork software

### 4.2.3 Analysis of the Testbed

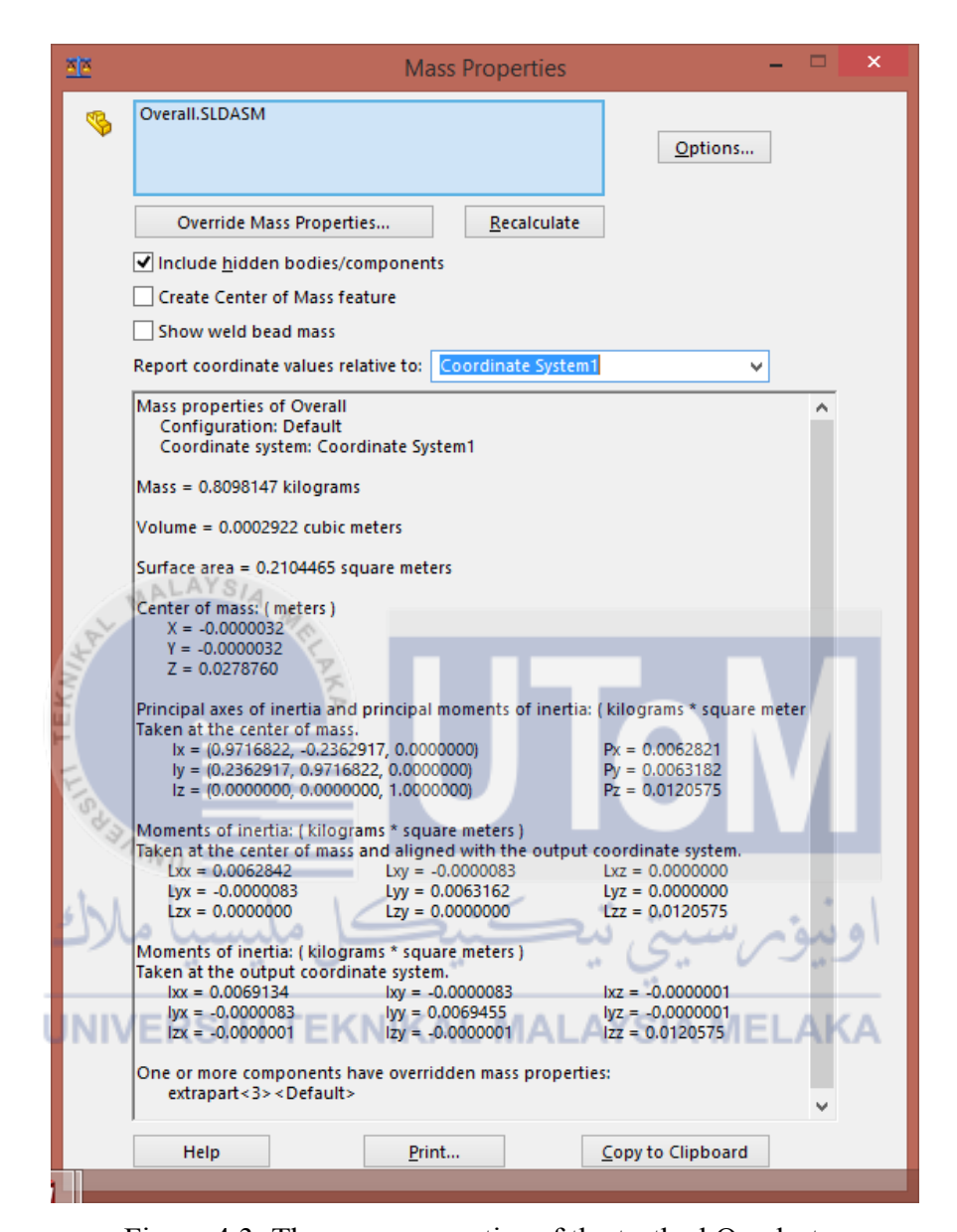


Figure 4.3: The mass properties of the testbed Quadrotor

From the Figure 4.3, it shows the mass properties of the testbed shown in Figure 4.1 which is drawn using Solidwork software. This mass properties is able to identify the mass, volume and total surface area of the testbed. Besides that, it also show the center of mass of the testbed. There are two types of moment of inertia shown where one of it is taken at the center of mass and aligned with the output coordinate system and the other is taken at the output coordinate system. Both of the moment of inertia is slightly the same is

due to the difference of center of mass and the origin. The moment of the inertia that is taken at the center of mass and aligned with the output coordinate system.

On the other hand, the uptrust force of the testbed itself is computed using the Solidwork Flow Simulation. The uptrust force is computed by giving an input of the average velocity. The Figure 4.4 showed that the result of a flow simulation of a given average velocity in an excel file.

### propeller.SLDPRT [Project(1) [flow test 1]] Goal Name Unit Averaged Value | Minimum Value | Maximum Value | Progress [%] | Use In Convergence | Delta Value Criteria 0.198048311 [N] 0.198017586 0.245978856 0.04626127 0.046619728 SG Force (Y) 1 0.214699086 100 Yes 8 Iterations: 120 9 Analysis interval: 54

Figure 4.4: Result for one of the flow simulation test

MALAYSIA

The goal name consist of various types of force that can be measured during the flow simulation test such as the force that is acting in the direction of x,y or z. Thus, the upthrust force is the upward force that is the force that acting in the direction of y. The angular velocity is depends on the average angular velocity that is found in the experiment of force-lift and rotor's speed test. Table 4.2 shows the average speed with the range from 0 to 7057 RPM given to generate the upthrust force of a propeller while the percentage speed % and the duty cycle of the propeller are calculated. The table of the results of the thrust force with the given angular velocity are shown in Table 4.2.

		<u> </u>	Č	Č	•
Duty	Percentage	Mass	Force,	Speed	Angular
Cycle	Speed (%)	Average	F (N)	Average	Velocity,
		(kg)		(RPM)	Ω (rad/s)
40	0.00	0.0000	0.0000	0	0.00
50	21.24	0.0000	0.1980	1499	156.97
60	38.43	0.0000	0.6540	2712	284.00
70	51.82	0.0000	1.1690	3657	382.96
80	59.40	0.0000	1.5300	4192	438.99
90	66.98	0.0000	1.9470	4727	495.01
100	74.69	0.0000	2.3950	5271	551.98
110	84.71	0.0000	3.0790	5978	626.01
120	90.66	0.0000	3.5160	6398	670.00
130	94.59	0.0000	3.8080	6675	699.00
140	100.00	0.0000	4.2460	7057	739.01

Table 4.2: The force generated with a given angular velocity

The Table 4.2 is then plotted into graph of force generated against the duty cycle calculated. The red-dotted line indicates the gradient of the graph while the blue line indicated the upthrust force generated with a given average speed.

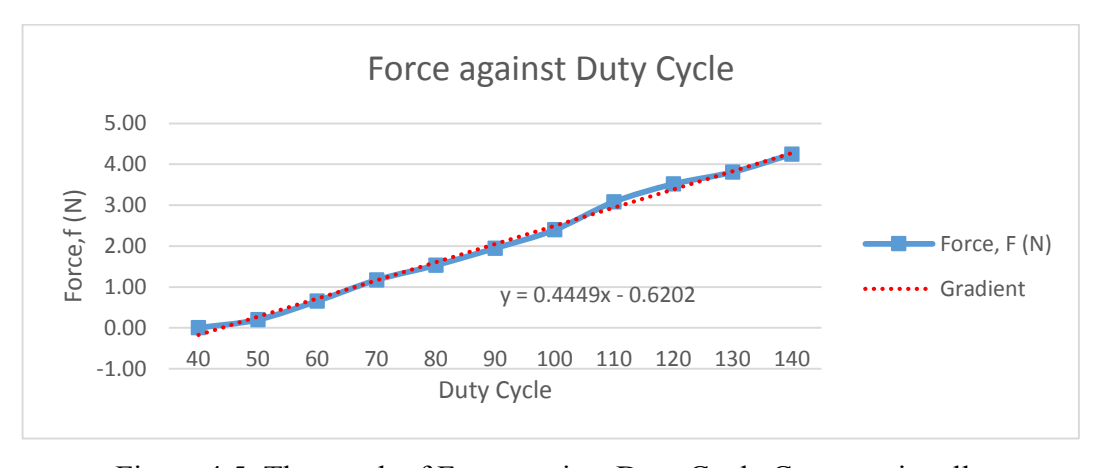


Figure 4.5: The graph of Force against Duty Cycle Computationally

(3.38)

From the Figure 4.5, the equation of the gradient and the equation 2.1 is used to calculate the results. The results are plotted in the Table 4.3. This simulation test is conducted to identify the value of the thrust force, b, and the drag force, d, of the drawn Quadrotor in Solidwork software shown in Figure 4.1. The results shown in Table 4.3 are input into the mathematical model of the Quadrotor system.

Table 4.3: Results of the simulation on testing the thrust force and drag force

Result	Value	Unit	Parameter
F	4.246	N	Force
b	7.775 x 10 <sup>-6</sup>	Ns²	Thrust Force
Ω	739.01	rad/s	Angular Velocity
d	1.2213 x 10 <sup>-5</sup>	Nms²	Drag Force
a	0.4449	N	Force for each motor

### 4.2.4 Mathematical Model of Quadrotor

Equation of motion

$$\ddot{x} = (-c\phi s\theta c\varphi - s\phi s\varphi)2.198$$

$$\ddot{y} = (-c\phi s\theta c\varphi + s\phi c\varphi)2.198 \tag{3.39}$$

$$\ddot{z} = g - (c\phi c\theta)2.198\tag{3.40}$$

$$\ddot{\phi} = \frac{1}{0.00628} \tau_{\phi} \text{ ERSITI TEKNIKAL MALAYSIA MELAKA}$$
 (3.41)

$$\ddot{\theta} = \frac{1}{0.00631} \tau_{\theta} \tag{3.42}$$

$$\ddot{\varphi} = \frac{1}{0.01206} \tau_{\varphi} \tag{3.43}$$

The input equation to the Quadrotor are given by:

$$u_{roll} = 9.6566 \times 10^{-6} (-\omega_2^2 + \omega_4^2)$$
(3.44)

$$u_{pitch} = 9.6566 \times 10^{-6} (-\omega_1^2 + \omega_3^2)$$
(3.45)

$$u_{yaw} = 1.2213 \times 10^{-5} (-\omega_1^2 - \omega_3^2 + \omega_2^2 + \omega_4^2)$$
(3.46)

$$u_{throttle} = 4.8852 \times 10^{-5} (\omega_1^2 + \omega_2^2 + \omega_3^2 + \omega_4^2)$$
(3.47)

Finally, the state-space representation of the Quadrotor as follows:

$$\begin{bmatrix} x_1 \\ x_2 \\ x_3 \\ x_4 \\ x_5 \\ x_6 \\ x_7 \\ x_8 \\ x_9 \\ x_{10} \\ x_{11} \\ x_{12} \end{bmatrix} = \begin{bmatrix} \dot{x} \\ \dot{y} \\ \dot{z} \\ \dot{x} \\ \dot{y} \\ \dot{z} \\ \dot{\phi} \\ \dot{\phi}$$

where  $u_1$  is  $u_{throttle}$ ,  $u_2$  is  $u_{roll}$ ,  $u_3$  is  $u_{pitch}$  and  $u_4$  is  $u_{yaw}$ .

UNIVERSITI TEKNIKAL MALAYSIA MELAKA

### 4.3 Results of Physical Realisation Experiments

This part contains results from four different experiments such as the physical measurement experiment, force-life and speed test, bifilar pendulum experiment and the complementary filter test. These experiments are conducted to achieve the objective that is to physically model the Quadrotor system.

### 4.3.1 Results of Physical Measurement

Table 4.4: The physical measurement of the respective components based on description

Description	Parameter		Unit				
Description	Tarameter	1st	2nd	3rd	Average		
Overall mass Quadrotor	$m_{total}$	0.838	0.837	0.838	0.837667	kg	
Mass of mechanical parts of  Quadrotor	$m_{mp}$	0.607	0.607	0.607	0.607000	kg	
Mass of battery	$m_b$	0.171	0.171	0.171	0.171000	kg	
Mass of a motor	$m_m$	0.052	0.052	0.052	0.052000	kg	
Mass of a propeller	$m_p$	0.011	0.011	0.011	0.011000	kg	
Mass of Quadrotor upper and lower base with frames attached	М	0.347	0.346	0.346	0.346333	kg	
Length of a frame	$l_f$	0.19	0.192	0.192	0.191333	m	
Length of a motor to centre of  Quadrotor	$l_{mtc}$	0.20	0.198	0.199	0.197667	m	
Length of a motor to opposite motor	$l_{mtm}$	0.397	0.399	0.396	0.397333	m	
Radius of Quadrotor base	$R_b$	0.065	0.068	0.07	0.067667	m	

The Quadrotor size can varies from mini to big scale system. The testbed is a small scale type as illustrated in Figure 4.1. The testbed is symmetrical in both x and y axis. The physical properties of the Quadrotor such as the weight and the length is the main influence in the modelling of the Quadrotor because it will affect the moment of inertia, thrust force and drag force of the Quadrotor.

These values shown in Table 4.4 can be considered acceptable due to it is a small scale Quadrotor as the weight of the Quadrotor is very important that will cause the system to be unstable. Furthermore, the value of parameter is very important and must be very accurate as it will cause difference on the modelling to be used for analysis. Therefore, the parameter is taken for three times to increase the accuracy of the measurement.

### 4.3.2 Results of Force-lift and Rotor's Speed Test

The force-lift test is conducted to identify the value of the thrust force, b, and the drag force, d, the Quadrotor system. Each motor is taken into account for testing in order to determine an accurate value of the forces that is calculated using the Newton's Second Law. The graph is then plotted to determine to the gradient of the force and the expected behaviour for each motor.

UNIVERSITI TEKNIKAL MALAYSIA MELAKA

### 4.3.2.1 Motor 1

Table 4.5: The results of force-lift test for motor 1

		Mass				Speed				Angular	
Duty Cycle	Percentage Speed (%)	1st test (kg)	2nd test (kg)	3rd test (kg)	Average (kg)	Force, F (N)	1st test (RPM)	2nd test (RPM)	3rd test (RPM)	Average (RPM)	Velocity, Ω (rad/s)
40	0.00	0.000	0.000	0.000	0.000	0.000	0	0	0	0	0.00
50	21.24	0.063	0.059	0.054	0.059	0.576	1473	1502	1522	1499	156.97
60	38.43	0.099	0.104	0.097	0.100	0.981	2754	2698	2684	2712	284.00
70	51.82	0.152	0.158	0.163	0.158	1.547	3684	3657	3630	3657	382.96
80	59.40	0.221	0.209	0.213	0.214	2.103	4174	4197	4205	4192	438.99
90	66.98	0.270	0.269	0.273	0.271	2.655	4699	4730	4752	4727	495.01
100	74.54	0.340	0.339	0.341	0.340	3.335	5259	5268	5253	5260	550.83
110	84.71	0.403	0.398	0.401	0.401	3.931	5970	6001	5963	5978	626.01
120	90.66	0.453	0.459	0.451	0.454	4.457	6393	6404	6397	6398	670.00
130	94.59	0.499	0.497	0.501	0.499	4.895	6671	6684	6670	6675	699.00
140	100.00	0.539	0.559	0.520	0.539	5.291	7059	7049	7063	7057	739.01

From the Table 4.5, the results is then plotted into graph of force-lift against the duty cycle of Motor 1 that is shown in Figure 4.6. Hence, the graph of the angular velocity against the duty cycle for motor 1 is also plotted and shown in Figure 4.7. The red-dotted line for both in Figure 4.6 and Figure 4.7 represents the gradient of the graph plotted.

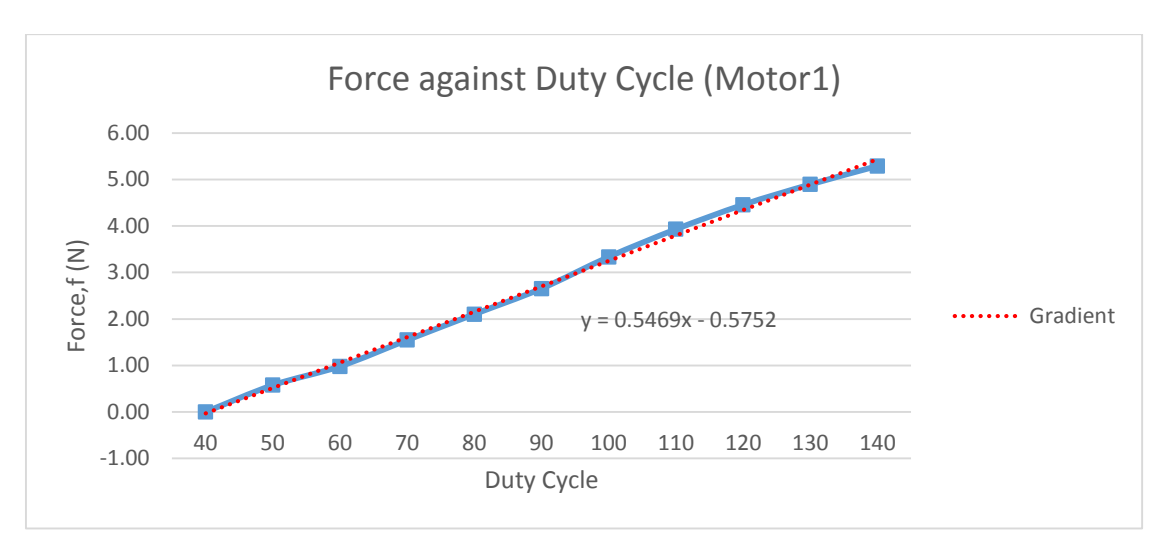


Figure 4.6: The graph of Force against Duty Cycle for Motor 1

From the Figure 4.6, the equation of the gradient and the equation 2.1 is used to calculate the results. The results are plotted in the Table 4.6 whereby the results shown are used to calculate the overall trust force and drag force of the Quadrotor system.

Table 4.6: Results of the simulation on testing the thrust force for Motor 1

Result	Value	Unit	Parameter
F PAINT	5.291	N	Force
b	9.688 x 10 <sup>-6</sup>	Ns <sup>2</sup>	Thrust Force
Ω	739.01	rad/s	Angular Velocity
aUNIVER	0.5469	MALAYSIA MI	Force from motor

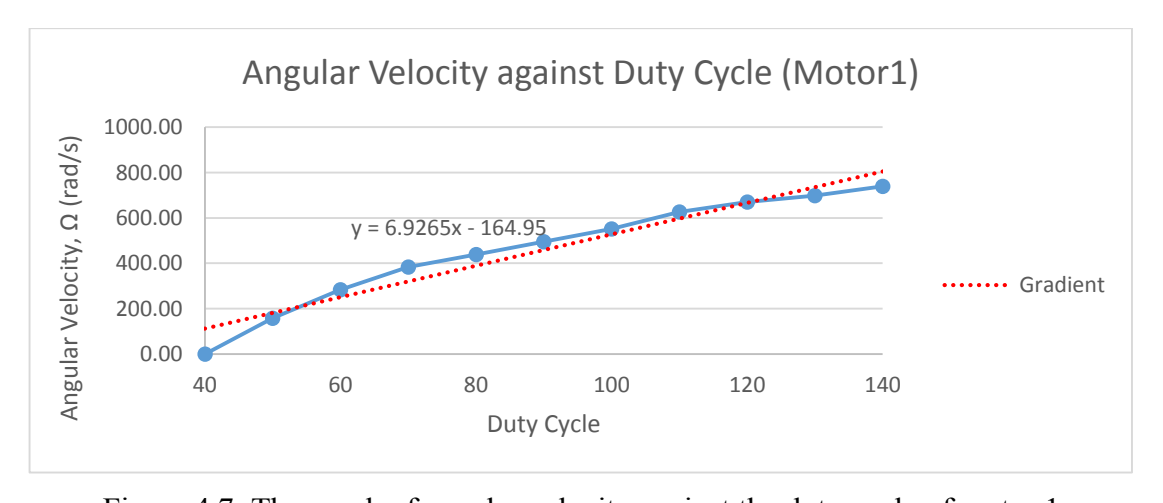


Figure 4.7: The graph of angular velocity against the duty cycle of motor 1

# 4.3.2.2 Motor 2

Table 4.7: The results of the force-lift test for motor 2

		Mass						Sp	eed		Angular		
Duty Cycle	Percentage Speed (%)	1st test (kg)	2nd test (kg)	3rd test (kg)	Average (kg)	Force, F (N)	1st test (RPM)	2nd test (RPM)	3rd test (RPM)	Average (RPM)	Velocity, Ω (rad/s)		
40	0.00	0.000	0.000	0.000	0.000	0.000	0	0	0	0	0.00		
50	21.34	0.062	0.060	0.061	0.061	0.599	1499	1512	1504	1505	157.60		
60	38.43	0.102	0.111	0.097	0.103	1.014	2701	2719	2710	2710	283.79		
70	51.84	0.159	0.158	0.160	0.159	1.560	3673	3662	3633	3656	382.86		
80	59.59	0.226	0.219	0.213	0.219	2.152	4202	4202 4207		4202	440.03		
90	66.93	0.269	0.271	0.272	0.271	2.655	4717 4722		4721	4720	494.28		
100	74.40	0.329	0.337	0.345	0.337	3.306	5249	5241	5251	5247	549.46		
110	84.70	0.401	0.411	0.407	0.406	3.986	5966	5972	5981	5973	625.49		
120	90.81	0.448	0.451	0.460	0.453	4.444	6397	6404	6411	6404	670.63		
130	94.68	0.492	0.503	0.499	0.498	4.885	6666	6687	6678	6677	699.21		
140	100.00	0.510	0.542	0.549	0.534	5.235	7042 7051		7051 7063		738.48		

From the Table 4.7, the results is then plotted into graph of force-lift against the duty cycle of Motor 1 that is shown in Figure 4.8. Hence, the graph of the angular velocity against the duty cycle for motor 1 is also plotted and shown in Figure 4.9. The red-dotted line for both in Figure 4.8 and Figure 4.9 represents the gradient of the graph plotted.

Force from motor

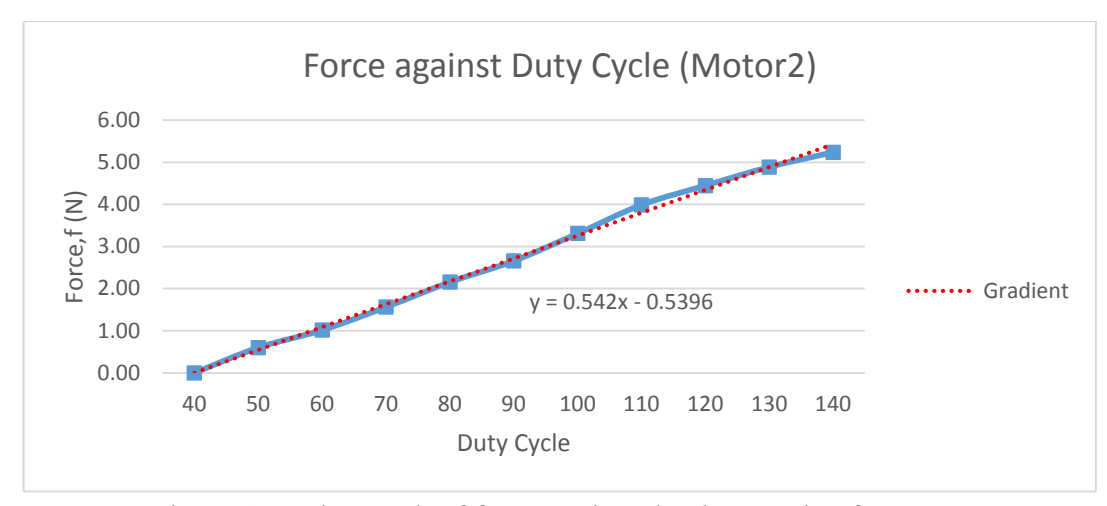


Figure 4.8: The graph of force against the duty cycle of motor 2

From the Figure 4.8, the equation of the gradient and the equation 2.1 is used to calculate the results. The results are plotted in the Table 4.8 whereby the results shown are used to calculate the overall trust force and drag force of the Quadrotor system.

	The state of the s		
Result	Value	Unit	Parameter
F	5.235	N	Force
b SAINI	9.599 x 10 <sup>-6</sup>	$Ns^2$	Thrust Force
0 /	738 48	rad/s	Angular Velocity

Table 4.8: Results of the simulation on testing the thrust force for Motor 2

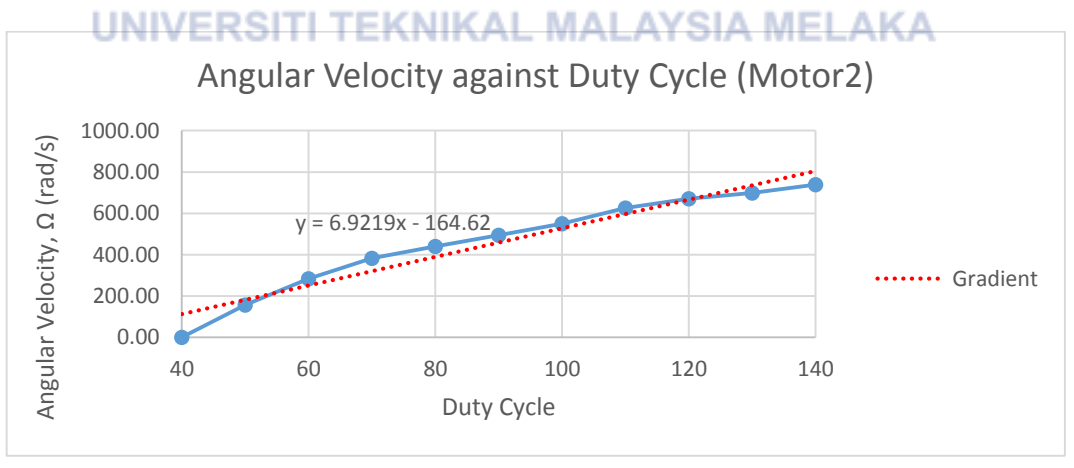


Figure 4.9: The graph of angular velocity against the duty cycle for motor 2

# 4.3.2.3 Motor 3

Table 4.9: The results of the force-lift test for motor 3

	Mass							Sp	eed		Angular			
Duty Cycle	Percentage Speed (%)	1st test (kg)	2nd test (kg)	3rd test (kg)	Average (kg)	Force, F (N)	1st test (RPM)	2nd test (RPM)	3rd test (RPM)	Average (RPM)	Velocity, Ω (rad/s)			
40	0.00	0.000	0.000	0.000	0.000	0.000	0	0	0	0	0.00			
50	21.18	0.062	0.056	0.054	0.057	0.562	1467	1498	1520	1495	156.56			
60	38.50	0.108	0.103	0.100	0.104	1.017	2732	2703	2719	2718	284.63			
70	51.78	0.151	0.158	0.161	0.157	1.537	3665	3667	3633	3655	382.75			
80	59.47	0.218	0.209	0.206	0.211	2.070	4188	4195	4211	4198	439.61			
90	66.95	0.268	0.266	0.271	0.268	2.632	4688	4735	4755	4726	494.91			
100	74.46	0.340	0.339	0.341	0.340	3.335	5257	5268	5243	5256	550.41			
110	84.76	0.389	0.404	0.399	0.397	3.898	5983	5994	5972	5983	626.54			
120	90.57	0.453	0.459	0.452	0.455	4.460	6394	6398	6387	6393	669.47			
130	94.50	0.499	0.503	0.491	0.498	4.882	6675	6671	6667	6671	698.59			
140	100.00	0.543	0.555	0.523	0.540	5.301	7061	7042 7074		7059	739.22			

From the Table 4.9, the results is then plotted into graph of force-lift against the duty cycle of Motor 1 that is shown in Figure 4.10. Hence, the graph of the angular velocity against the duty cycle for motor 1 is also plotted and shown in Figure 4.11. The red-dotted line for both in Figure 4.10 and Figure 4.11 represents the gradient of the graph plotted.

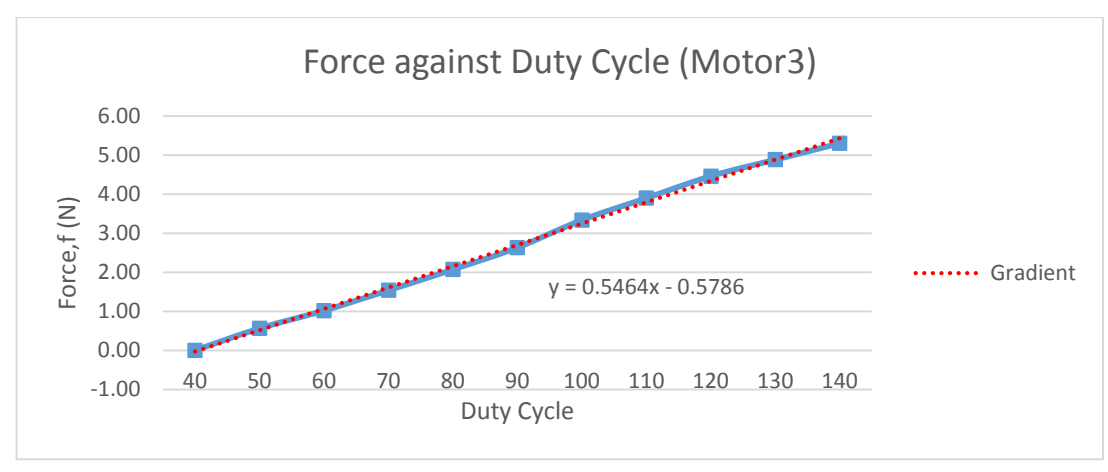


Figure 4.9: The graph of force against the duty cycle of motor 3

From the Figure 4.9, the equation of the gradient and the equation 2.1 is used to calculate the results. The results are plotted in the Table 4.10 whereby the results shown are used to calculate the overall trust force and drag force of the Quadrotor system.

MALAYSIA

Table 4.10: Results of the simulation on testing the thrust force for Motor 3

Result	Value	Unit	Parameter
F	5.301	N	Force
b Fee	9.701 x 10 <sup>-6</sup>	$Ns^2$	Thrust Force
Ω	739.22	rad/s	Angular Velocity
ا ملاك	0.5464	سىت <sub>3</sub> ك	Force from motor

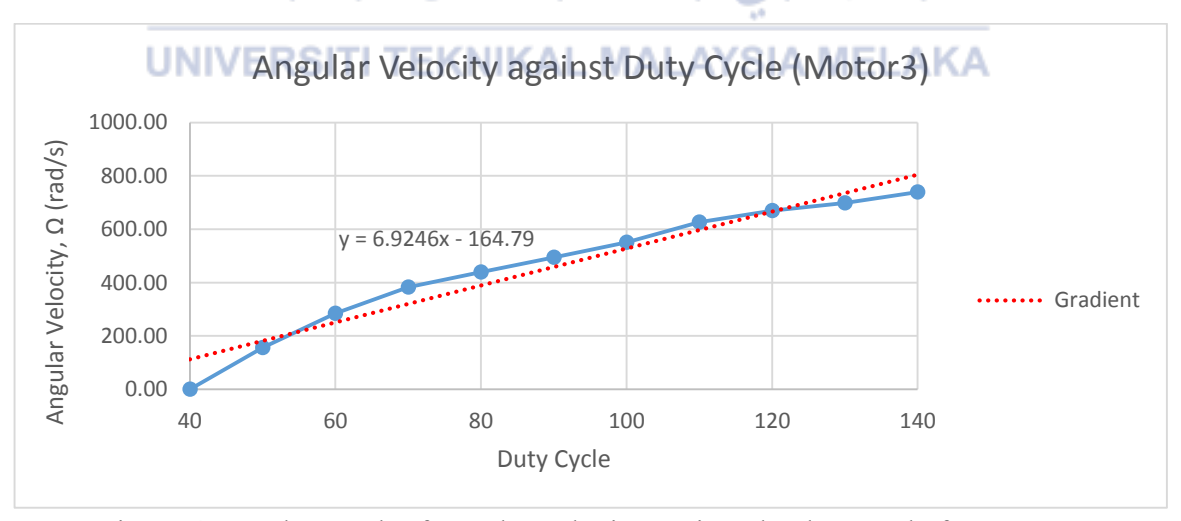


Figure 4.10: The graph of angular velocity against the duty cycle for motor 3

# 4.3.2.3 Motor 4

Table 4.11: The results of the force-lift test for motor 4

			N	⁄lass				Sp	peed		Angular
Duty Cycle	Percentage Speed (%)	1 <sup>st</sup> test (kg)	2 <sup>nd</sup> test (kg)	3 <sup>rd</sup> test (kg)	Average (kg)	Force, F (N)	1 <sup>st</sup> test (RPM)	2 <sup>nd</sup> test (RPM)	3 <sup>rd</sup> test (RPM)	Average (RPM)	Velocity, $\Omega$ (rad/s)
40	0.00	0.000	0.000	0.000	0.000	0.000	0	0	0	0	0.00
50	21.31	0.067	0.059	0.062	0.063	0.615	1491	1504	1520	1505	157.60
60	38.41	0.106	0.101	0.099	0.102	1.001	2727	2704	2708	2713	284.10
70	51.76	0.159	0.154	0.161	0.158	1.550	3662	3659	3647	3656	382.86
80	59.39	0.221	0.208	0.215	0.215	2.106	4188	4201	4196	4195	439.30
90	66.89	0.265	0.268	0.279	0.271	2.655	4716	4733	4726	4725	494.80
100	74.33	0.329	0.334	0.326	0.330	3.234	5 <b>2</b> 54	<b>52</b> 54	<b>5</b> 245	5251	549.88
110	84.65	0.391	0.406	0.402	0.400	3.921	5980	5985	5975	5980	626.22
120	90.56	0.452	0.449	0.455	0.452	4.434	6399	6395	6397	6397	669.89
130	94.39	0.498	0.501	0.496	0.498	4.889	6661	6669	6674	6668	698.27
140	100.00	0.536	0.543	0.539	0.539	5.291	7064	7059	7069	7064	739.74

From the Table 4.11, the results is then plotted into graph of force-lift against the duty cycle of Motor 1 that is shown in Figure 4.12. Hence, the graph of the angular velocity against the duty cycle for motor 1 is also plotted and shown in Figure 4.13. The red-dotted line for both in Figure 4.12 and Figure 4.13 represents the gradient of the graph plotted.

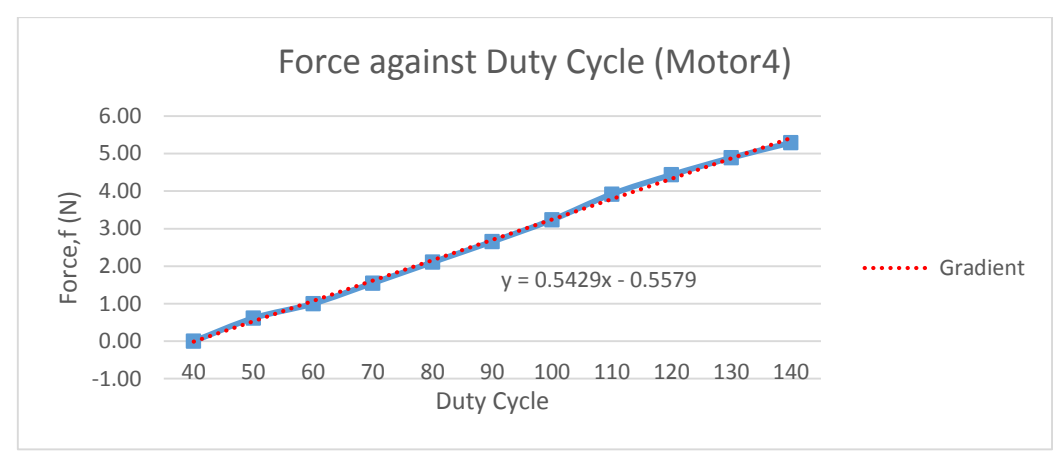


Figure 4.12: The graph of force against the duty cycle for motor 4

From the Figure 4.12, the equation of the gradient and the equation 2.1 is used to calculate the results. The results are plotted in the Table 4.12 whereby the results shown are used to calculate the overall trust force and drag force of the Quadrotor system.

Table 4.12: Results of the simulation on testing the thrust force for Motor 4

Result	Value	Unit	Parameter
F	5.291	N	Force
b	9.669 x 10 <sup>-6</sup>	Ns <sup>2</sup>	Thrust Force
Ω	739.74	rad/s	Angular Velocity
a July (	0.5429	N	Force from motor

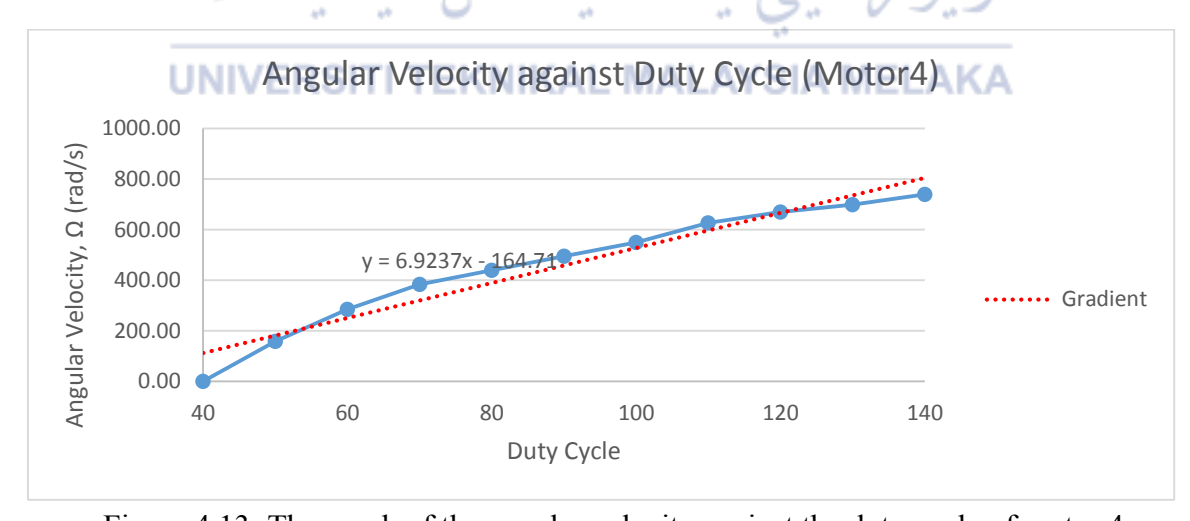


Figure 4.13: The graph of the angular velocity against the duty cycle of motor 4

Parameter	Value	Unit	Remark
$a_1$	0.5469	N	Thrust Factor Motor1
$a_2$	0.5419	N	Thrust Factor Motor2
$a_3$	0.5464	N	Thrust Factor Motor3
$a_4$	0.5429	N	Thrust Factor Motor4
b	$6.0722 \times 10^{-5}$	Ns <sup>2</sup>	Average Thrust factor
d	$1.518 \times 10^{-5}$	Nms <sup>2</sup>	Drag Factor

Table 4.13: Result of the Force-Lift Test

The speed of the rotor measured depends on the value of the servo angle in the simulation of Arduino. As the speed of the rotor increases by 10 in terms of duty cycle, the value of servo angle increases. In the process of this experiment, the angle of the propeller's angular velocities and the force generated are measured by using tachometer and weighting scale respectively. Based on the theory of momentum, the upward force of the propeller is proportional to the square of the rotational speed of the propeller. Thus, the upward force, known as the thrust force, *b*, of the maximum speed for each and every motor is calculated with the equation 2.1.

$$F = b\Omega^2$$

where the F is the thrust force and  $\Omega$  is the angular velocity.

# UNIVERSITI TEKNIKAL MALAYSIA MELAKA

The trend of the angular velocity for each motor are very similar which is due to the same power input. Although the motor 2 has a minimal difference with other motors, the performance is still can be accepted due to it had experience an accident previously. The similarity of the trend causes the thrust factor of each rotor is almost the same.

It can be seen in the results of every motor that the starting pulse that enable the rotation of the motor is at 50 with the maximum PWM signal of 130. Any increment of the PWM signal larger than 130 will generate the same angular velocity. In overall, the duty cycle of 50 PWM is equal to 21 percent of the speed of the motor which can be considered as the minimum speed to start the rotation of the motor.

## 4.3.3 Results of Bifilar Pendulum Experiment

From the Table 4.4 that is the table of the results for the physical measurement, the moment of inertia can be calculated with the results of the Bifilar Pendulum Experiment. This experiment is conducted to determine the moment of inertia for x, y and z axis by measuring the time taken for the Quadcopter to complete its  $360^{\circ}$  swing with two ropes with equal length using a stopwatch. The system is rotated manually using hand and then it is released to rotate by itself. The Quadrotor starts to swing when released about the axis of system due to the tension of the ropes tied onto the system. The time taken for the experiment is used to calculate the inertia of the system together with the results shown in Table 4.14.

Table 4.14:	Result of	the Bifilar	Pendulum	Experiment							
	Time taken for the period of swing										
Movement	1st test (s)	2nd test (s)	3rd test (s)	Average (s)							
Yaw	4.16	4.11	4.02	4.10							
Roll	0.42	0.39	0.42	0.41							
Pitch	0.44	0.38	0.41	0.41							

NIVERSITI TEKNIKAL MALAYSIA MELAKA

Figure 4.14: The graph of yaw of the Quadrotor system

The Figure 4.14 shows the graph of the gyroscope's output when The Quadrotor is swinging in yaw direction. The blue line indicates the swinging of the Quadrotor while the red line is the ideal line for the yaw swinging of Quadrotor.

Calculation of moment of inertia using results from experiment,

$$I_{yaw} = \left[\frac{T_n}{2\pi}\right] \frac{mgR^2}{L}$$

$$I_{yaw} = \left[\frac{4.10}{2\pi}\right] \frac{(0.838)(9.81)(0.12)^2}{0.4}$$

$$I_{yaw} = 0.1931kgm^2/s$$

$$I_{roll} = \left[\frac{T_n}{2\pi}\right] \frac{mgR^2}{L}$$

$$I_{roll} = \left[\frac{0.41}{2\pi}\right] \frac{(0.838)(9.81)(0.12)^2}{0.4}$$

$$I_{roll} = 0.01931kgm^2/s$$

$$I_{pitch} = \left[\frac{T_n}{2\pi}\right] \frac{mgR_b^2}{L}$$

$$I_{pitch} = \left[\frac{0.41}{2\pi}\right] \frac{(0.838)(9.81)(0.12)^2}{0.4}$$

$$I_{pitch} = 0.01931kgm^2/s$$

Theoretically,

$$I_{y} = I_{x} = \frac{2MR_{b}^{2}}{5} + 2l_{f}^{2}m_{m}$$

$$I_{y} = I_{x} = \frac{2(0.3463)(0.0677)^{2}}{5} + 2(0.1913)^{2}(0.052)$$

$$I_{y} = I_{x} = 0.00444kgm^{2}/s$$

$$I_{z} = \frac{2MR_{b}^{2}}{5} + 4l_{f}^{2}m_{m}$$

$$I_{z} = \frac{2(0.3463)(0.0677)^{2}}{5} + 4(0.1913)^{2}(0.052)$$

$$I_{z} = 0.00825kgm^{2}/s$$

Table 4.15: The moment of Inertia through calculation and theoretically

Parameter	Value	Unit	Remarks
$I_{yaw}$	0.1931	kgm²/s	Experiment Moment of inertia yaw
$I_{roll}$	0.01931	kgm²/s	Experiment Moment of inertia roll
$I_{pitch}$	0.01931	kgm²/s	Experiment Moment of inertia pitch
$I_{x}$	0.00444	kgm²/s	Theoretical Moment of inertia along x-axis
$I_{y}$	0.00444	kgm²/s	Theoretical Moment of inertia along y-axis
$I_z$	0.00825	kgm²/s	Theoretical Moment of inertia along z-axis
М	0.34633	kg	Overall Mass without motor
$R_b$	0.06766	m	Radius of Quadrotor base
m	0.83767	kg	Overall mass Quadrotor
$m_m$	0.0520	kg	Mass of Motor
$l_f$	0.1913	М	Length of frame
g	9.81	$m/s^2$	Gravitational force

It can be seen in Table 4.15 that the moment of inertia of theoretical differs from the experimented moment of inertia. This is due to there are many disturbance during the process of experiment while the theoretical moment of inertia is an ideal value of the Quadrotor system. Besides, it can be also due to the thickness of the rope used as it can make difference on the time taken for the Quadrotor to complete a full 360° swing. Both of the moment of inertia about roll and pitch axes are assumed to be same as the system are symmetrical but the value is different with the moment of inertia about yaw due to the different of number of frame taken into account during the experiment. There are four frames involved in the process of yawing while there are only two frames involved for the process of rolling and pitching. Although there are slight difference between theoretical, the moment of inertia value is used as the input equation in the controller's algorithm.

### 4.3.4 Mathematical Model of Quadrotor

$$\ddot{x} = (-c\phi s\theta c\varphi - s\phi s\varphi)2.6 \tag{3.38}$$

$$\ddot{y} = (-c\phi s\theta c\varphi + s\phi c\varphi)2.6 \tag{3.39}$$

$$\ddot{z} = g - (c\phi c\theta)2.6 \tag{3.40}$$

$$\ddot{\Phi} = \frac{1}{0.01931} \tau_{\Phi} \tag{3.41}$$

$$\ddot{\theta} = \frac{1}{0.01931} \tau_{\theta} \tag{3.42}$$

$$\ddot{\varphi} = \frac{1}{0.1931} \tau_{\varphi} \tag{3.43}$$

The input equation to the Quadrotor are given by:

$$u_{roll} = 1.2003 \times 10^{-5} (-\omega_2^2 + \omega_4^2) \tag{3.44}$$

$$u_{pitch} = 1.2003 \times 10^{-5} (-\omega_1^2 + \omega_3^2)$$
 (3.45)

$$u_{yaw} = 1.518 \times 10^{-5} (-\omega_1^2 - \omega_3^2 + \omega_2^2 + \omega_4^2)$$
 (3.46)

$$u_{throttle} = 6.0722 \times 10^{-5} (\omega_1^2 + \omega_2^2 + \omega_3^2 + \omega_4^2)$$
 (3.47)

Finally, the state-space representation of the Quadrotor as follows:

where  $u_1$  is  $u_{throttle}$ ,  $u_2$  is  $u_{roll}$ ,  $u_3$  is  $u_{pitch}$  and  $u_4$  is  $u_{yaw}$ .

### 4.4 Analysis for Mathematical Model of Quadrotor

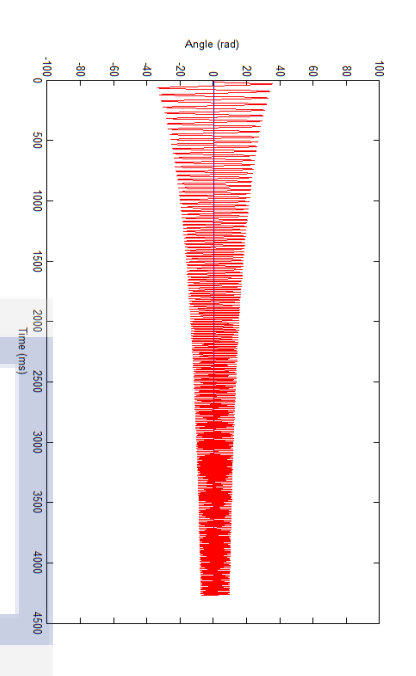
This part is to analyse the mathematical models of the Quadrotor system that obtained computationally and physically. By obtaining the open loop test of the system, they can be compared on which method of mathematical modelling is more accurate and better. The coding that is written in MATLAB and the block diagram in SIMULINK. The results of the thrust force and the moment of inertia together with the results of physical measurement are included in the coding of the MATLAB where this coding represents the plant of the Quadrotor system. The analysis is done as the plant is given inputs of desire roll, pitch, yaw and z direction and produces output of the open loop system for each of every direction and movement.

# 4.4.1 Computationally Method of Mathematical Modelling

MALAYSIA

The state space representation that created using the results of the moment of inertia, the thrust force and physical measurement is analysed using MATLAB with SIMULINK which is shown in APPENDIX D and APPENDIX E. The APPENDIX D shows the coding of MATLAB that represents the plant of the Quadrotor system and the APPENDIX E shows the block diagram where the purple box on the left is the desired inputs and the white blocks on the right represents the outputs comparing with the desired inputs. The plant is named as 'Computationally' is being substituted with the state space representation.

The desired input for the direction of z-axis is 1 m while the direction of x-axis and y-axis are 0 m. Besides, the desired input for the pitch angle is 16° while the desired input for the yaw and roll are 16° and 16° respectively. The output of the plant is represented with red line while the blue line indicates the input of the plant which is given as a constant value together with the analysis of the respective graph. The outputs and the inputs are in the unit of radian (rad).



i. RiseTime

: 0.7650 s

Figure 4.15: The graph of output and input in pitch movement for computational modelling

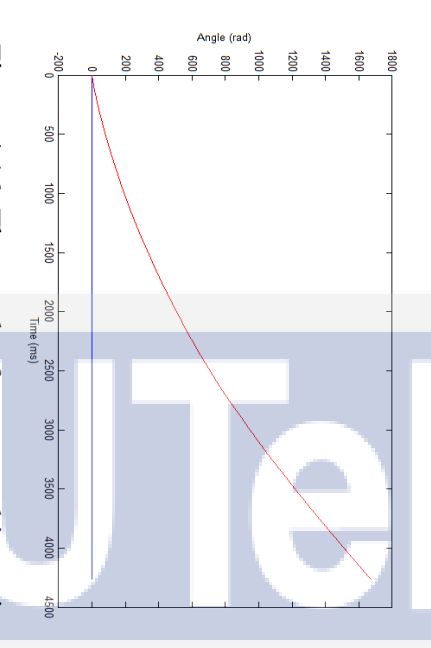


Figure 4.16: The graph of output and input in yaw movement for computational modelling

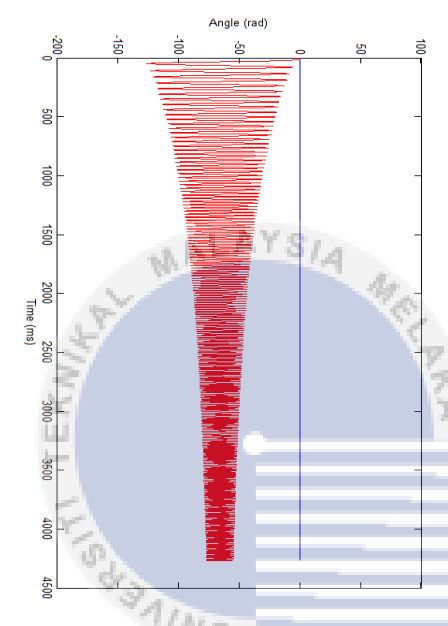


Figure 4.17: The graph of output and input in roll movement for computational modelling

 ii. SettlingTime
 : 4.2706e+03 s

 iii. SettlingMin
 : -33.6246 s

 iv. SettlingMax
 : 33.9801 s

 v. Overshoot
 : 1.6292e+03 %

 vi. Undershoot
 : 1.8216e+03 %

 vii. Peak
 : 35.4202 rad

 viii. PeakTime
 : 33 s

i. RiseTime: 3.0948e+03 s

ii. SettlingTime : 4.2183e+03 s

iii. SettlingMin : 1.5071e+03 s

iv. SettlingMax : 1.6744e+03 s

v. Overshoot : 0 % vi. Undershoot : 0 %

vii. Peak : 1.6744e+03 rad

viii. PeakTime : 4271 s

i. RiseTime : 10.7303 sii. SettlingTime : 4.2701e+03 s

iv. SettlingMax : -6.2236 s

Ξ:

SettlingMin

-126.5932 s

v. Overshoot : 127.9428 % vi. Undershoot : 0.4824 %

vii. Peak : 126.5932 rad

viii. PeakTime : 49 s

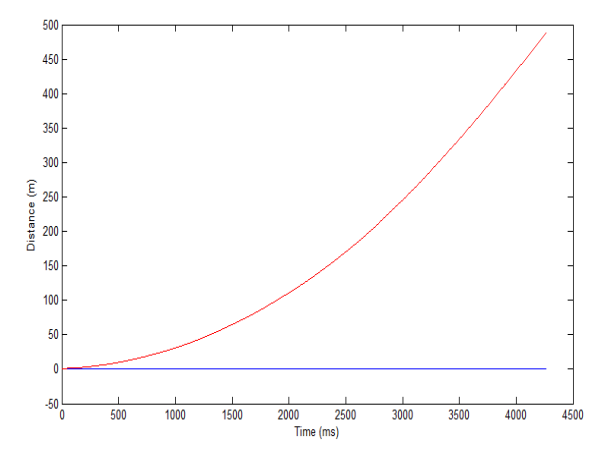


Figure 4.18: The graph of output and input in z direction for computational modelling

i. RiseTime : 2.7353e+03 s

ii. SettlingTime: 4.2266e+03 s

iii. SettlingMin : 440.9098 s

iv. SettlingMax: 489.6404 s

v. Overshoot : 0 %

vi. Undershoot : 0 %

vii. Peak : 489.6404 m

viii. PeakTime : 4271 s

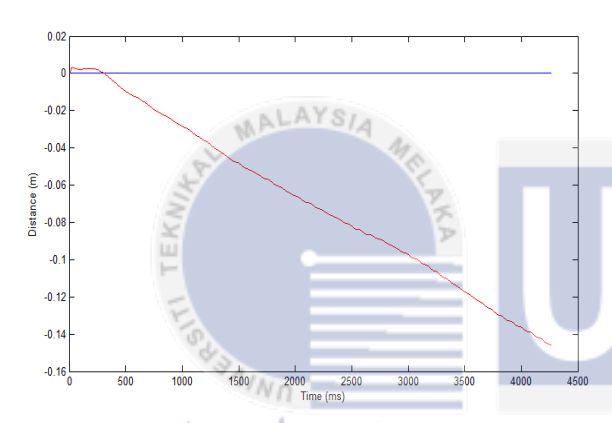


Figure 4.19: The graph of output and input in y direction for computational modelling

RiseTime : 3.2064e+03 s

ii. SettlingTime: 4.1946e+03 s

iii. SettlingMin : -0.1462 s

iv. SettlingMax : -0.1316 s

v. Overshoot : 0 %

vi. Undershoot : 1.9732 %

vii. Peak : 0.1462 m

viii. PeakTime : 4271 s

# UNIVERSITI TEKNIKAL MALAYSIA MELAKA

i.

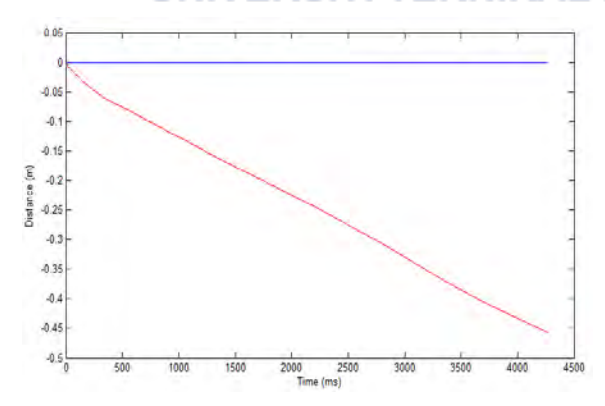


Figure 4.20: The graph of output and input in x direction for computational modelling

- i. RiseTime : 3.5261e+03 s
- ii. SettlingTime: 4.1728e+03 s
- iii. SettlingMin : -0.4573 s
- iv. SettlingMax : -0.4117 s
- v. Overshoot : 0 %
- vi. Undershoot : 0 %
- vii. Peak : 0.4573 m
- viii. PeakTime : 4271 s

## 4.4.2 Physically Method of Mathematical Modelling

The state space representation that created using the results of the moment of inertia, the thrust force and physical measurement is analysed using MATLAB with SIMULINK that is shown in APPENDIX F and APPENDIX G respectively which is likely the same as for the process of analysis for the computationally model of the Quadrotor system. The APPENDIX F shows the coding of MATLAB that represents the plant of the Quadrotor system and the APPENDIX G shows the block diagram where the purple box on the left is the desired inputs and the white blocks on the right represents the outputs comparing with the desired inputs. The plant that is named as 'Physically' is being substituted with the state space representation.

The desired input for the direction of z-axis is 1 m while the direction of x-axis and y-axis are 0 m. Besides, the desired input for the pitch angle is 16° while the desired input for the yaw and roll are 16° and 16° respectively. The output is represented with red line while the blue line indicates the desired input of the plant which is given as a constant value together with the analysis of the respective graph. The outputs and the inputs are in the unit of radian (rad).

UNIVERSITI TEKNIKAL MALAYSIA MELAKA

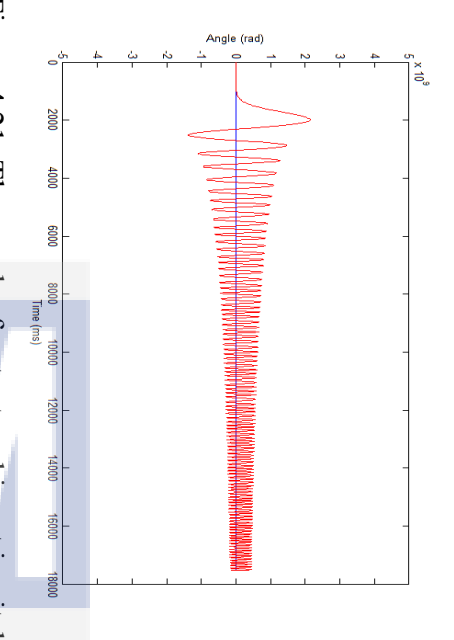


Figure 4.21: The graph of output and input in pitch movement for physical modelling

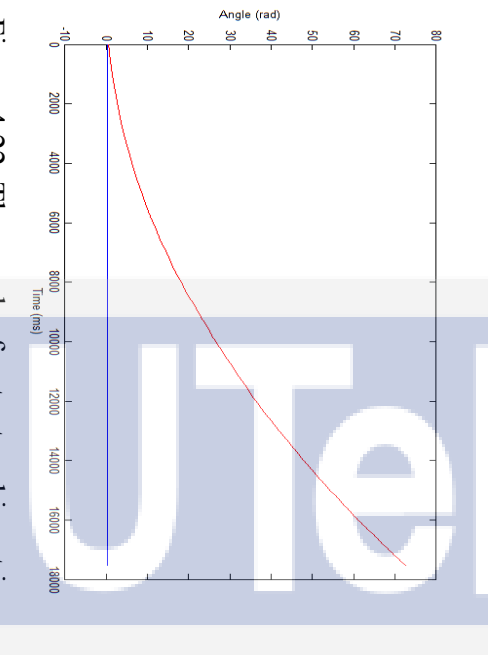


Figure 4.22: The graph of output and input in yaw movement for physical modelling

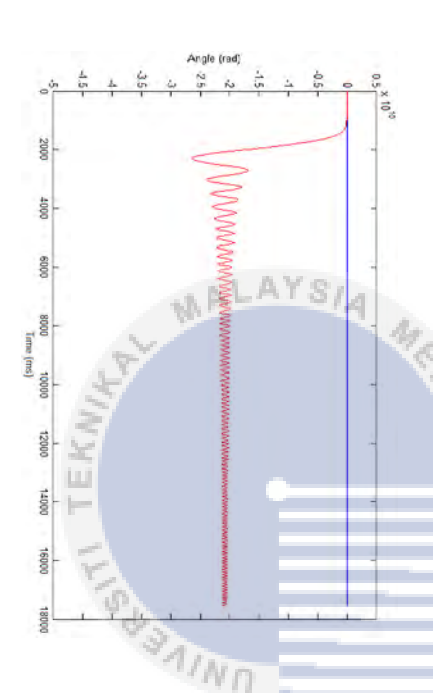


Figure 4.22: The graph of output and input in roll movement for physical modelling

VII. VIII. Ξ: ≦. Λ. Ξ: < Peak **PeakTime** Undershoot SettlingMax SettlingMin SettlingTime Overshoot RiseTime : 824 s : 4.5871e+03 s : 217.7929 % : 263.5641 % : 2.2792e+06 s : 3.8046e+06 rad : 174.3340 s -3.8046e+06 s

VIII \_≦ V1: Peak Undershoot Overshoot SettlingMax SettlingMin SettlingTime RiseTime **PeakTime** : 4592 s : 0 % : 0 % : 22.8572 rad : 4.5443e+03 s : 22.8572 s : 20.6021 s : 3.2727e+03 s

< SettlingTime SettlingMax SettlingMin Undershoot Overshoot RiseTime : 0 % : 4.5831e+03 s : 4.0472e+07 s : 25.3749 % : 2.5827e+07 s : 245.0355 s

VIII. ¥11. Peak **PeakTime** : 993 s : 4.0472e+07 rad

≦.

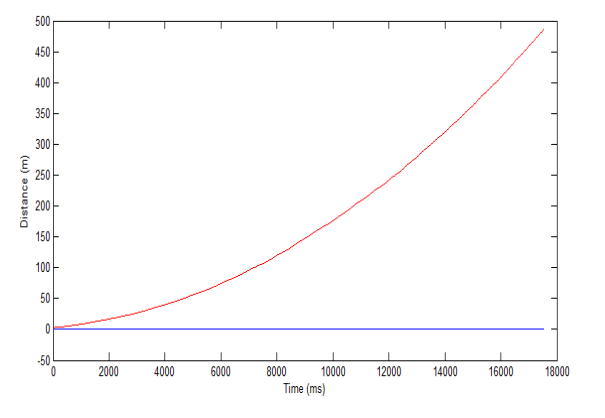


Figure 4.23: The graph of output and input in z direction for physical modelling

i. RiseTime : 3.2556e+03 s

ii. SettlingTime: 4.5446e+03 s

iii. SettlingMin : 438.2502 s

iv. SettlingMax: 486.6952 s

v. Overshoot : 0 %

vi. Undershoot : 0 %

vii. Peak : 486.6952 m

viii. PeakTime : 4592 s

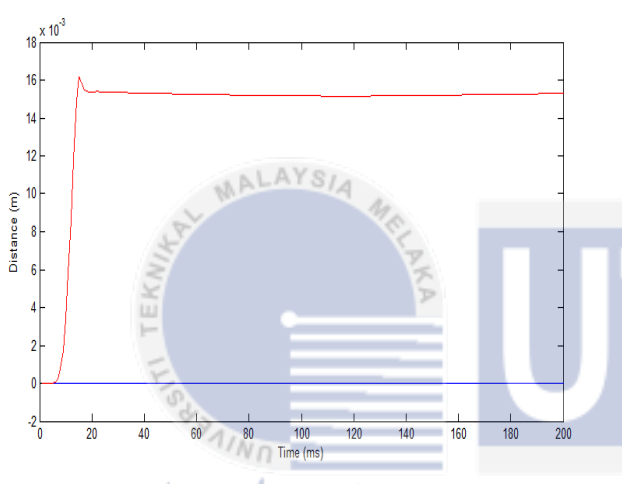


Figure 4.24: The graph of output and input in y direction for physical modelling

i. RiseTime : 3.9010e+03 s

ii. SettlingTime: 4.5190e+03 s

iii. SettlingMin: 2.8486 s

iv. SettlingMax: 3.1643 s

v. Overshoot : 0 %

vi. Undershoot : 0 %

vii.

viii.

Peak : 3.1643 m

PeakTime : 4592 s

# UNIVERSITI TEKNIKAL MALAYSIA MELAKA

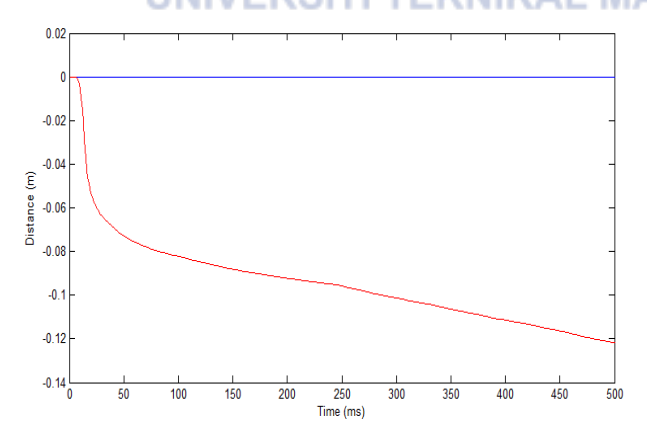


Figure 4.25: The graph of output and input in x direction for physical modelling

i. RiseTime : 4.0183e+03 s

ii. SettlingTime : 4.5174e+03 s

iii. SettlingMin : -2.6289 s

iv. SettlingMax : -2.3663 s

v. Overshoot : 0 %

vi. Undershoot : 0 %

vii. Peak : 2.6289 m

viii. PeakTime : 4592 s

### 4.4.3 Comparison for the Outputs

The trend of the graph shown in Figure 4.14 is likely the same as the graph shown in Figure 4.20 for the movement of pitch of the Quadrotor system. Both of the graphs show that the amplitude for output value is decreasing exponentially until it reaches the desired input. In other words, both of the output is in the underdamped case  $(0 < \zeta < 1)$  whereby the decay rate is small till it reach the desired output which is in  $0^{\circ}$ . Besides that, the graph of Figure 4.15 and Figure 4.21 show that the movement of the yaw for the Quadrotor system increases exponentially even though  $0^{\circ}$  is given as the desired output value. Furthermore, the Figure 4.16 and Figure 4.22 represents the output of the movement of roll for the Quadrotor system. The Quadrotor system that is modelled computationally rolls in and the Quadrotor system that is modelled physically rolls in negative degree rolls in negative direction that final value around -60 rad and -2 rad respectively.

For the direction of x, the trend of the x-direction is decreasing proportionally for the computationally modelling that shown in Figure 4.19 while the trend of the x-direction is decreasing exponentially for the physical modelling that shown in Figure 4.25. Besides that, the movement in y direction is decreasing proportionally for the computationally modelling that is shown in Figure 4.18 while the trend of the y-direction is increasing for the physically modelling which is shown in Figure 4.24. On the other hand, the distance in z-direction is increasing exponentially for both of the modelling which is shown in Figure 4.17 and Figure 4.23 respectively. The analysis for every graph is computed out with the help of MATLAB using the coding of *stepinfo()*. By using this coding, the performance of the modelling such as the rise time, settling time, the maximum and minimum of the settling time, the overshoot and undershoot, the peak time and the peak are computed. The difference in the value of performance of the modelling in terms of the rise time, peak time and the other results are due to the difference in the moment of inertia and the thrust force that measured from the Quadrotor system.

In the process of modelling computationally, the parameter of the Quadrotor in the Solidwork is very important as the more accurate the drawing, the better of the results on the moment of inertia and the thrust force. Any lack of accuracy in drawing will results the output of the Quadrotor system analysed in MATLAB. Thus, parameter of the Quadrotor is

very important. On the other hand, the experiments conducted in the process of the modelling physically should be handled well and precise. This is due to any error occurred will give different results on the final output of the plant. In the physical measurement, the parameter of the Quadrotor testbed should be measured properly and precisely as the results are used for the calculation for moment of inertia and the trust force. The measurement of the rotor's speed must be accurate as the results are used for the computation of the thrust force in the process of modelling computationally. All of the above should be taken care properly in order to prevent any mistake or changes in the results of the analysis which is the output of the plant.



#### **CHAPTER 5**

#### **CONCLUSION**

#### 5.1 Conclusion

The main objective for this project is to physically and computationally modelling a small scale Quadrotor system. The assembly of the Quadrotor is being drawn using Solidworks CAD design software. The dimensions of the Quadrotor is based on the testbed developed by previous FYP student. The assembly is being converted into SimMechanics Toolbox via SimMechanics Link for simulation and generating parameters needed for modelling such as the moment of inertia and the thrust force on the propellers. On the other hand, four experiments were conducted such as the physical measurement, force-lift and speed test, bifilar pendulum experiment and complementary filter. The physical measurement is conducted to obtain the important length and weight of respective components to be used for the next experiments. Last but not least, the body of the Quadrotor is being estimated by using complementary filter that used accelerometer and gyroscope in the IMU to estimate the current position of the body for the Quadrotor and remove unwanted noises. There are important parameter are being measured and calculated to be used for modelling. There are two types of modelling which produces similar parameters, such as the moment of inertia and the thrust force but different output of the Quadrotor system. This is due to computational modelling is based on the software limitations such as the joints while the physical realisation experiments experienced errors such as parallex error. Although physical modelling shows a lower steady state error, the computational modelling is still acceptable with its minor steady state error. Thus, both of the modelling method will produce a different transient response of the open loop Quadrotor system whereby it can be used to produce a suitable controller.

### **5.2 Suggestion for Future Work**

The results can be further improved in terms of accuracy. In terms of computationally modelling of the Quadrotor system, the drawing of the Quadrotor in the Solidwork software should be more accurately with a more precise measurement of parameter of the Quadrotor system. The more precise the drawing of the Quadrotor system in Solidwork, the more accurate the moment of inertia and the thrust force generated through simulation. On the other hand, the physical realization experiment should be conducted in a safer environment whereby increasing the numbers of precautionary steps in order to get a more precise and accurate results of moment of inertia and the thrust force for each motor. Both of the modelling have their own advantages and disadvantages due to their own limitations. Furthermore, an increase number of parameter taken into account in order to make the state space representation produced by the MATLAB to increase the efficiency and accuracy of the specific modelling. Thus, by obtaining a better method of modelling will lead to a production of a better controller which is the next step after producing the plant of a system.

UNIVERSITI TEKNIKAL MALAYSIA MELAKA

### REFERENCES

- [1] Bousbaine, A. Wu, H. & Poyi, G., Modelling And Simulation of A Quadrotor Helicopter., vol., no., p.1 6
- [2] P.Lambermont. AviaStar. Retrieved December 2012 Available: http://www.aviastar.org/helicopters\_eng/convertawings.php.

MALAYSIA

- [3] "Portal Eastern Sabah Security Command". Retrieved October, 2014 Available: http://esscom.gov.my/esszone-dan-esscom/
- [4] Wurm, L, Legge, G, Isenberg, L & Luebker, A, Color Improves Object Recognition in Normal and Low Vision, vol 19, no, p.903 904
- [5] D. Ardema, Mark, Newton-Euler Dynamics. Springer Science + Business Media, Inc.; 2005.
- [6] Ginsberg, Jerry , Engineering Dynamics. Cambridge University Press ; Vol . 10. 2008.

# UNIVERSITI TEKNIKAL MALAYSIA MELAKA

- [7] "SimMechanics". Retrieved September, 2014 Available: http://www.mathworks.com/help/physmod/sm/index.html
- [8] "SimMechanics Link" ". Retrieved September, 2014 Available: http://www.mathworks.com/help/physmod/smlink/ug/product-overview.html#brrkqtv-1
- [9] Jun, J , Juntong, Q , Dalei, S , Jianda, H , Control Platform Design and Experiment of a  $Quadrotor \ , p.2974-2979$
- [10] Rodic, A, Mester, G, The Modeling and Simulation of an Autonomous Quad-Rotor Microcopter in a Virtual, p.107 120

- [11] Fernando, H , De Silva, A , Dilshan, K ,Munasinghe , S , Modelling, Simulation and Implementation of a Quadrotor UAV , p.207-211
- [12] Gautam, D, Ha, C, Control of a Quadrotor Using a Smart Self-Tuning Fuzzy PID Controller, p.1 7
- [13] Naidoo, Y, Stopforth, R, Bright, G, Quad-rotor Unmanned Aerial Vehicle Helicopter Modelling & Control, p.139 147
- [14] Mustafa, M, Modelling and Decentralized Adaptive Tracking Control of a Quadrotor UAV, p.293 299
- [15] Jinpeng, Y, Zhihao, C, Qing, L, Yingxun, W, Self-tuning PID Control Design for Quadrotor UAV Based on Adaptive Pole Placement Control, p.233 120
- [16] Yasir Amir, M, Abbas, V, Modeling and Neural Control of Quadrotor Helicopter,
  p.35 45
- [17] Ameho, Y, Niel, F, Defay, F, Biannic, J, Berard, C, Adaptive Control for Quadrotors, p.5396 5401
- [18] Kalpesh, S, Dutt, B, Modh, H, Quadrotor An unmanned Aerial Vehicle, vol 2, no 1, p.1299 1302
- [19] Orsag, M, Bogdan, S, Influence of Forward and Descent Flight on Quadrotor Dynamics, p.141 155
- [20] Edward, P , Pounds, I , Design, Construction and Control of a Large Quadrotor Micro Air Vehicle , p.56 57
- [21] Tefay, B, Eizad, B, Crosthwaite, P, Singh, S, & Postula, A, Design of an Integrated Electronic Speed Controller for Compact Robotic Vehicles, vol, no, p.2 3

- [22] Güçlü, A, Attitude and Altitude Control of an Outdoor Quadrotor, M.S. thesis, Atilim University, Turkey, July 2012.
- [23] Junior, J , Paula, J , Leandro, G , & Bonfim, M , Brazilian Journal of Instrumentation and Control , Stability Control of a Quad-Rotor Using a PID Controller , vol , no ISSN 2318-4531, p.15 20
- [24] Mohd Ariffanan, M , Husain, A, R, Danapalasingam, K, A , Fuzzy Supervisory
   Backstepping Controller for Stabilization of Quadrotor Unmanned Aerial Vehicle , p.1
   5
- [25] P.Chmelar, Building and Controlling the Quadcopter, Faculty of Electrical Engineering and Computer Science, University of Padubice, Tech. Rep. 95, 532 10,



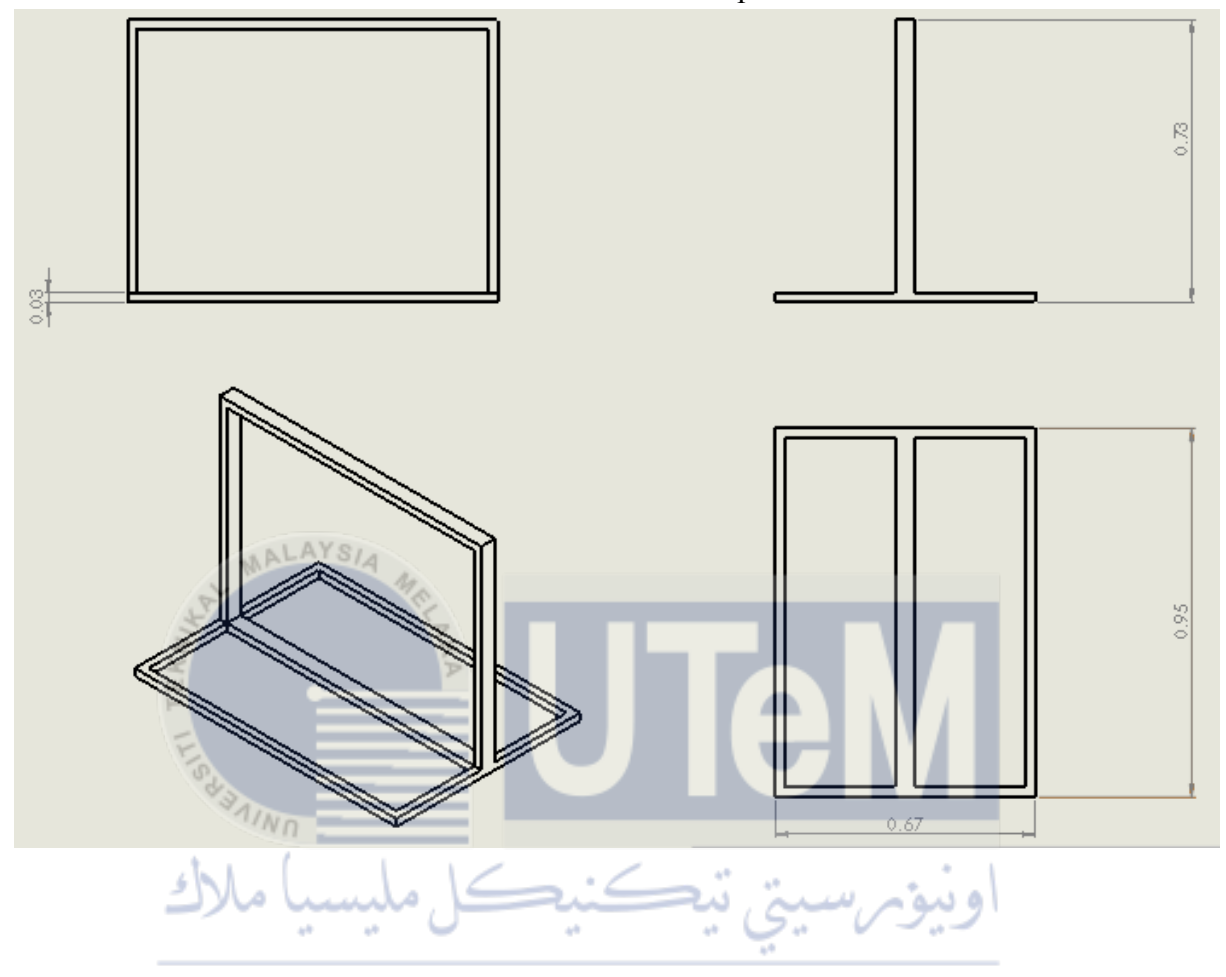
# APPENDIX A

# **Gantt Chart of the Research**

														We	eek													
Activity							20	14													20	)15						
	1	2	3	4	5	6	7	8	9	10	11	12	13	14	1	2	3	4	5	6	7	8	9	10	11	12	13	14
Chapter 1: Introduction AYS/A																												
(i) Research Background	4,																											
(ii) Motivation	18																											
(iii) Problem Statement		N																										
(iv) Objectives		47	6																									
(v) Scope														1														
Chapter 2: Literature Review																												
(i) Principles and Theories																												
(ii) Jounals Review							•									/												
(iii) Summary of Review												L						L										
Chapter 3: Methodology																												
(i) Model Computationally																												
(ii) Model Physically				No.					g de	e de la companya della companya della companya de la companya della companya dell			49															
(iii) Analysis and Simulation	۵						J						7		1	1		7		4	'n.	در	A					
Chapter 4: Result		J	-				4						1		П	į,			1	-	1	, -	1					
(i) Assembly of Testbed															4.0													
(ii) Obtain related parameters			1			1									7							١.						
(iii) Physical Realisation Experiments			٨	7		Ĺ	٩		I	17	N	_/	H	r	2	7		Ш	Ш	L	Ρ	1	J	4				
(iv) Testing and Analysis																												
Chapter 5: Conclusion																												
(i) Conclusion																												
(ii) Future Work																												
Final Report																												

# APPENDIX B

The sketch of the testbench used in Bifilar Pendulum Experiment with the dimensions.

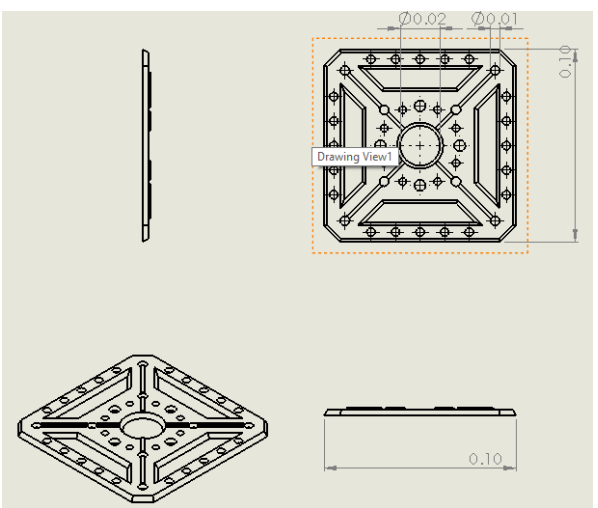


UNIVERSITI TEKNIKAL MALAYSIA MELAKA

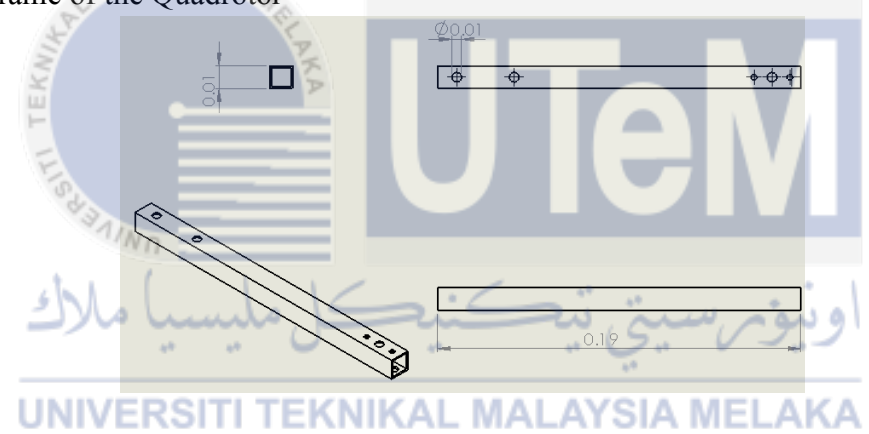
# APPENDIX C

The components of the Quadrotor with dimensions.

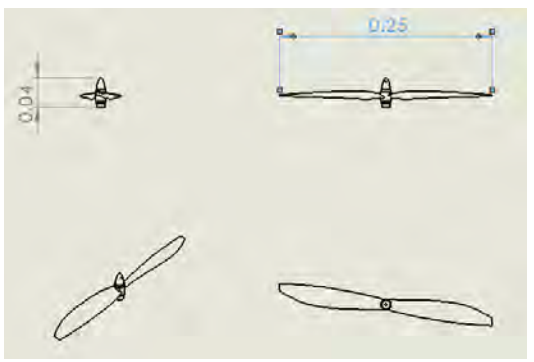
i.) The base of the Quadrotor



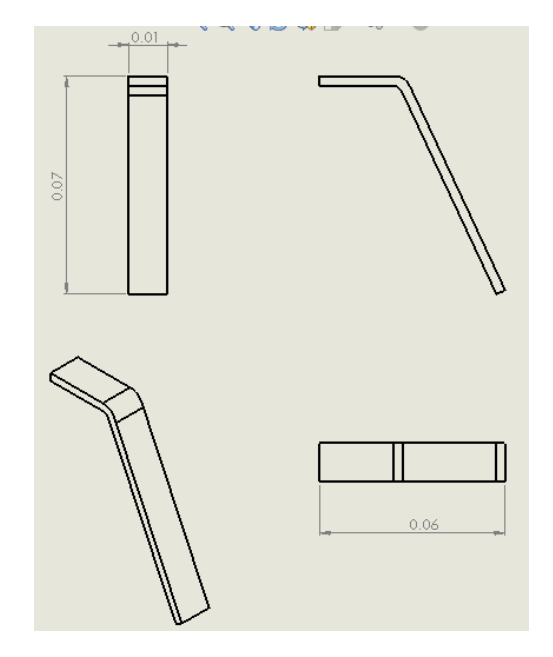
ii.) The frame of the Quadrotor



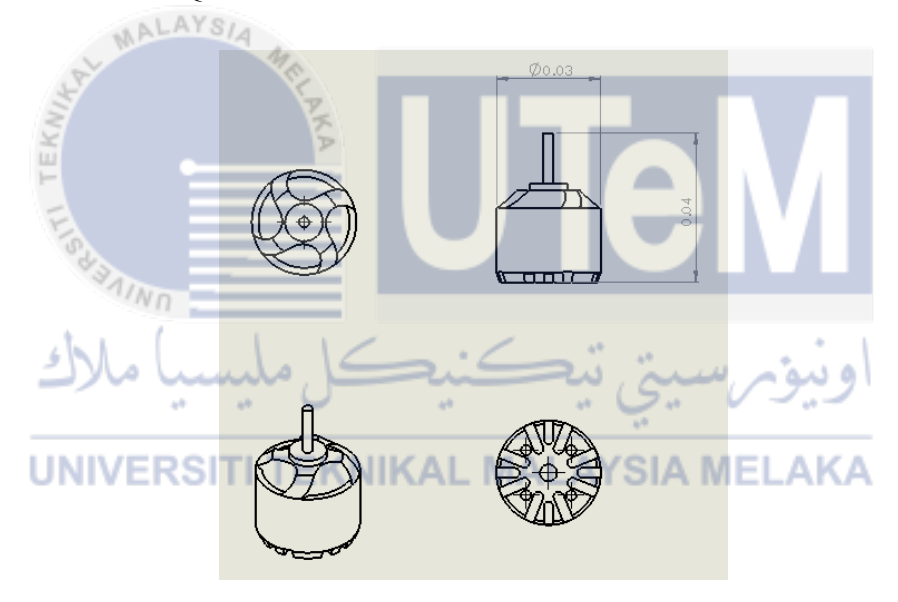
iii.) The propeller of Quadrotor



iv.) The landing gear of Quadrotor



# v.) The motor used in Quadrotor



All the measurements in the CAD design for all the components are in mm unit.

### APPENDIX D

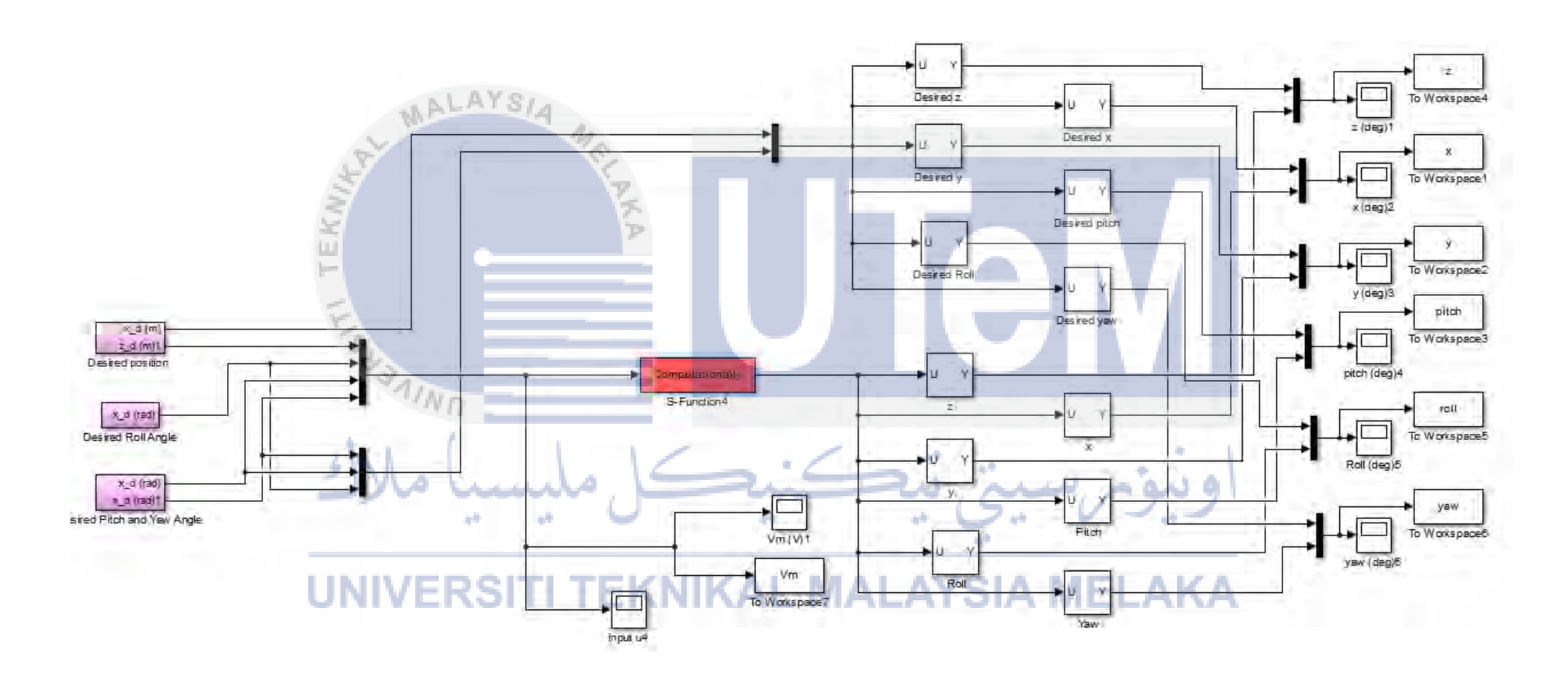
# MATLAB coding for Computational Modelling of Quadrotor System

```
function [sys,x0,str,ts] = Computationally(t,x,u,flag)
C = eye(12, 12);
switch flag,
 case 0,
    [sys,x0,str,ts]=mdlInitializeSizes();
 case 1,
    sys = mdlDerivatives(t,x,u);
 case 3,
    sys=mdlOutputs(t,x,C);
end
function [sys,x0,str,ts]=mdlInitializeSizes()
sizes = simsizes;
sizes.NumContStates = 12;
sizes.NumDiscStates = 0;
sizes.NumOutputs
                      = 12;
sizes.NumInputs = 4;
sizes.DirFeedthrough = 0;
sizes.NumSampleTimes = 1;
sys = simsizes(sizes);
x0=[0 \ 0 \ 1 \ 0 \ 0 \ 0.261 \ 0.261 \ 0.261 \ 0
                                        0]';
str = [];
ts=[0 0];
function sys=mdlDerivatives(t,x,u)
g = 9.81;
Ix = 0.00628;
Iy = 0.00631;
Iz = 0.01206;
L = 0.1975;
m = 0.8098147;
q = pi/180;

Jr = 3.01e-3;
                          EKNIKAL MALAYSIA MEL
b = 4.8852e-5;
d = 1.2213e-5;
T = [b \ b \ b; 0 \ b \ 0 \ -b; \ b \ 0 \ -b \ 0; \ d \ -d \ d \ -d];
uu = u;
os = inv(T)*u(1:4,1);
os = (os + abs(os))/2;
omega = sqrt(os(1)) - sqrt(os(2)) + sqrt(os(3)) - sqrt(os(4));
sys(1) = x(4);
sys(2) = x(5);
sys(3) = x(6);
sys(4) = -((cos(x(7))*sin(x(8))*cos(x(9)) + sin(x(7))*sin(x(9)))*uu(1))/m;
sys(5) = -((cos(x(7))*sin(x(8))*sin(x(9)) - sin(x(7))*cos(x(9)))*uu(1))/m;
sys(6) = g - ((cos(x(7))*cos(x(8)))*uu(1))/m;
sys(7) = x(10);
sys(8) = x(11);
sys(9) = x(12);
sys(10) = (x(11)*x(12)*(Iy-Iz)/Ix) - (Jr/Ix)*x(11)*omega+ (L/Ix)*uu(2);
sys(11) = (x(10)*x(12)*(Iz-Ix)/Iy) - (Jr/Iy)*x(10)*omega+ (L/Iy)*uu(3);
sys(12) = (x(10)*x(11)*(Ix-Iy)/Iz) + (1/Iz)*uu(4);
function sys=mdlOutputs(t,x,u,C)
C=eye(12,12);
sys=C*x
```

# APPENDIX E

# **Block Diagram for the Computational Modelling of Quadrotor System**



### APPENDIX F

## **MATLAB Coding for Physical Modelling of Quadrotor System**

```
function [sys,x0,str,ts] = Physically(t,x,u,flag)
C=eye(12,12);
switch flag,
 case 0,
    [sys,x0,str,ts]=mdlInitializeSizes();
 case 1,
    sys = mdlDerivatives(t, x, u);
 case 3,
    sys=mdlOutputs(t,x,C);
end
function [sys,x0,str,ts]=mdlInitializeSizes()
sizes = simsizes;
sizes.NumContStates = 12;
sizes.NumDiscStates = 0;
sizes.NumOutputs
                    = 12;
sizes.NumInputs
                     = 4;
sizes.DirFeedthrough = 0;
sizes.NumSampleTimes = 1;
sys = simsizes(sizes);
x0=[0\ 0\ 1\ 0\ 0\ 0\ 0.261\ 0.261\ 0.261\ 0\ 0\ 0]';
str = [];
ts=[0 0];
function sys=mdlDerivatives(t,x,u)
q = 9.81;
Ix = 0.01931;
Iy = 0.01931;
Iz = 0.1931;
L = 0.1975;
m = 0.8377;
q = pi/180;
Jr = 3.01e-3;
b = 6.0722e-5;
d = 1.518e-5;
T = [b b b; 0 b 0 -b; b 0 -b 0; d -d d -d];
uu = u;
os = inv(T)*u(1:4,1);
os = (os + abs(os))/2;
omega = sqrt(os(1)) - sqrt(os(2)) + sqrt(os(3)) - sqrt(os(4));
sys(1) = x(4);
sys(2) = x(5);
sys(3) = x(6);
sys(4) = -((cos(x(7))*sin(x(8))*cos(x(9)) + sin(x(7))*sin(x(9)))*uu(1))/m;
sys(5) = -((cos(x(7))*sin(x(8))*sin(x(9)) - sin(x(7))*cos(x(9)))*uu(1))/m;
sys(6) = g - ((cos(x(7))*cos(x(8)))*uu(1))/m;
sys(7) = x(10);
sys(8) = x(11);
sys(9) = x(12);
sys(10) = (x(11)*x(12)*(Iy-Iz)/Ix) - (Jr/Ix)*x(11)*omega+ (L/Ix)*uu(2);
sys(11) = (x(10)*x(12)*(Iz-Ix)/Iy) - (Jr/Iy)*x(10)*omega+ (L/Iy)*uu(3);
sys(12) = (x(10)*x(11)*(Ix-Iy)/Iz) + (1/Iz)*uu(4);
function sys=mdlOutputs(t,x,u,C)
C=eye(12,12);
sys=C*
```

# APPENDIX G

# **Block Diagram for Physical Modelling of Quadrotor System**

